

# Engineering and Characterization of an Enzyme Replacement Therapy for Classical Homocystinuria

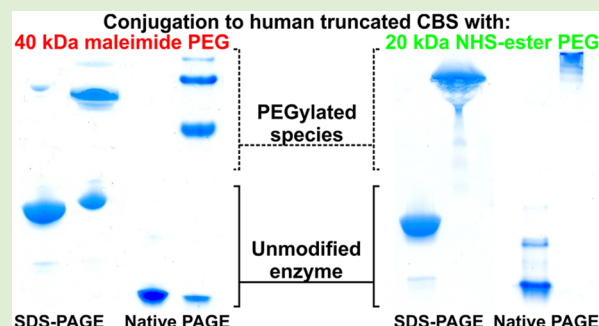
Tomas Majtan,<sup>\*,†</sup> Insun Park,<sup>†</sup> Richard S. Carrillo,<sup>†</sup> Erez M. Bublil,<sup>‡</sup> and Jan P. Kraus<sup>\*,†</sup>

<sup>†</sup>Department of Pediatrics, University of Colorado School of Medicine, Aurora, Colorado 80045, United States

<sup>‡</sup>Orphan Technologies Ltd., Rapperswil, CH-8640, Switzerland

## S Supporting Information

**ABSTRACT:** Homocystinuria due to loss of cystathionine beta-synthase (CBS) causes accumulation of homocysteine and depletion of cysteine. Current treatments are suboptimal, and thus the development of an enzyme replacement therapy based on PEGylated human truncated CBS (PEG-CBS) has been initiated. Attenuation of potency was observed, which necessitated a screen of several PEG-CBS conjugates for their efficacy to correct and maintain the plasma metabolite profile of murine homocystinuria after repeated administrations interrupted with washouts. We found that CBS coupling with maleimide PEG inconsistently modified the enzyme. In contrast, the PEG-CBS conjugate with 20 kDa N-hydroxysuccinimide-PEG showed very little loss of potency likely due to a reproducible PEGylation resulting in species modified with five PEGs per subunit on average. We developed assays suitable for monitoring the extent of CBS PEGylation and demonstrated a sustainable partial normalization of homocystinuria upon continuous PEG-CBS administration via osmotic pumps. Taken together, we identified the PEG-CBS conjugate suitable for manufacturing and clinical development.



## INTRODUCTION

Human cystathionine beta-synthase (CBS, EC 4.2.1.22) is a pivotal enzyme of sulfur amino acid metabolism, whose activity determines either recycling of the sulfur in the methionine cycle or its diversion into synthesis of cysteine through the transsulfuration pathway.<sup>1,2</sup> The critical intermediate of sulfur amino acid metabolism is the nonproteinogenic amino acid homocysteine (Hcy), which can be either converted back to methionine by an action of methionine synthase or betaine homocysteine methyltransferase or redirected by CBS to cysteine biosynthesis via the transsulfuration pathway. CBS is a pyridoxal-5'-phosphate-dependent homotetrameric hemeprotein, which catalyzes the condensation of Hcy with serine forming cystathionine (Cth) and water. Cth is subsequently hydrolyzed by the action of cystathionine gamma-lyase to cysteine (Cys) and alpha-ketobutyrate, which completes the conversion of the essential amino acid methionine to Cys. Activity of CBS, and thus the flux of sulfur through the transsulfuration pathway, is attenuated by the autoinhibitory function of the enzyme's C-terminal regulatory domain. Binding of S-adenosylmethionine to this domain results in a conformational rearrangement of the regulatory domain, subsequent release of the autoinhibitory block, and 4–5-fold activation of the enzyme.<sup>3</sup> A similar level of CBS activation can be achieved by removal of the C-terminal regulatory domain and consequent formation of a dimeric permanently activated human truncated enzyme (htCBS).<sup>4,5</sup>

Lack of CBS activity results in classical homocystinuria (HCU), an autosomal recessively inherited rare metabolic disorder.<sup>6</sup> The inactivation of CBS, chiefly due to the presence of missense pathogenic mutations, yields severe elevation of Hcy, methionine, and S-adenosylhomocysteine and conversely lack of Cth and decrease of Cys in plasma samples of HCU patients. These biochemical sequelae are accompanied by connective tissue disorders such as dislocated optic lenses, long and thin limbs and osteoporosis, thromboembolism, cognitive impairment, and other clinical symptoms.<sup>6</sup> Treatment of HCU is mostly symptomatic aimed at reduction of Hcy concentration in the plasma and tissues by protein-restricted diet with methionine-free L-amino acid supplementation.<sup>7</sup> This dietary intervention is often combined with betaine, which promotes the remethylation of Hcy back to methionine.<sup>8</sup> In addition, supplementation with the pyridoxal-5'-phosphate precursor pyridoxine (vitamin B<sub>6</sub>) was proven effective in roughly 50% of HCU patients by stimulating the residual CBS activity and thus relieving the clinical manifestation and relaxing the dietary regime.<sup>9</sup> Although methionine restriction is particularly effective in lowering plasma Hcy levels, a compliance of the HCU patients with the diet is quite poor with consequent manifestation of the symptoms.<sup>10</sup> Thus, there is a need for an alternative therapy that would not require a stringent diet but

Received: February 1, 2017

Revised: April 17, 2017

Published: April 21, 2017



would achieve similar reduction of Hcy levels and prevent onset or escalation of the clinical symptoms.

We have recently described an enzyme replacement therapy (ERT) for HCU using PEGylated htCBS.<sup>11</sup> We have shown that unmodified htCBS exhibited rapid clearance from the circulation of the mouse model of the disease (elimination half-life after IV administration was 2.7 h). PEGylation, that is, conjugation of protein of interest to one or more polyethylene glycol (PEG) moieties, is a well-recognized and accepted strategy to alter pharmacokinetic profiles of a variety of drugs and thereby improving their therapeutic potential.<sup>12–14</sup> Indeed, PEGylation of htCBS resulted in 6–11-fold longer elimination half-life of PEGylated htCBS after IV administration, improved plasma metabolic profile of murine homocystinuria in HO mice,<sup>15</sup> and rescued the CBS knockout mice<sup>16</sup> from neonatal lethality by preventing the liver damage.<sup>11</sup>

The goal of the present study was to design and characterize a PEG htCBS conjugate that would exhibit high reproducibility and control during manufacturing as well as display long-term efficacy. In the previous study, we showed that an introduction of the C15S point mutation to htCBS diminished formation of protein aggregates and higher order oligomers and improved PEGylation profile for the 20 kDa linear maleimide-activated PEG.<sup>11</sup> Here, we tested various htCBS C15S conjugates with either maleimide- or *N*-hydroxysuccinimide (NHS) ester-activated PEG (further referred as PEG-CBS) for their potency to correct metabolic profile of murine homocystinuria after multiple rounds of repeated administration interrupted with washout periods. This test allowed us to rank-order studied PEG-CBS conjugates based on their pharmacodynamics. In addition, we gained insight into reproducibility and consistency of PEG-CBS preparations, characterized the sites modified by the PEGs, and identified the assays useful to monitor and evaluate the extent of htCBS C15S PEGylation. As a result, we identified the most suitable PEG-CBS lead candidate for development of ERT for HCU.

## ■ EXPERIMENTAL SECTION

**Chemicals.** Unless stated otherwise, all materials were purchased from Sigma or Fisher Scientific. L-[<sup>14</sup>C]-serine was obtained from PerkinElmer Life Sciences.

**Animals.** All animal procedures were approved under animal protocol no. B-49414(03)1E by the University of Colorado Denver IACUC, which is an AAALAC-accredited (#00235), Public Health Service-assured (#A 3269–01), and USDA-licensed (#84-R-0059) institution. Human Only (HO) mice were previously generated in our laboratory<sup>15</sup> and propagated and genotyped as described previously.<sup>11</sup> Animals were maintained on extruded standard diet 2918 or 2919 (Harlan, CA, USA). A single-use lancet was used for blood collection by submandibular bleeding into Capiject T-MLHG lithium heparin (12.5 IU) tubes with gel (Terumo Medical Corporation, NJ, USA). Tubes were then centrifuged at 1200g for 10 min followed by transfer of plasma to 1.5 mL tubes and storage at –80 °C.

**Determination of Metabolite Concentrations.** Plasma metabolites, including total homocysteine (Hcy), total cysteine (Cys), cystathionine (Cth), were determined by stable-isotope-dilution gas chromatography mass spectrometry as previously described.<sup>17</sup> The analysis was performed in a blinded fashion without knowledge of the animal genotype or treatment regimen.

**HPLC Size Exclusion Chromatography (SEC-HPLC).** Various CBS and PEG-CBS preparations were separated on BioSEC-5 7.8 × 300 mm, 1000 Å pore size column (Agilent, CA, USA). Column was equilibrated and operated in 100 mM sodium phosphate pH 6.8, 150 mM NaCl at a flow rate of 1 mL/min at room temperature. Protein samples diluted in mobile phase to a final concentration of 2 mg/mL

were loaded on a column via 10 µL sample loop and detected using UV detector at wavelength of 225 nm. Chromatograms were recorded and analyzed using 32karat software (Beckman Coulter, CA, USA).

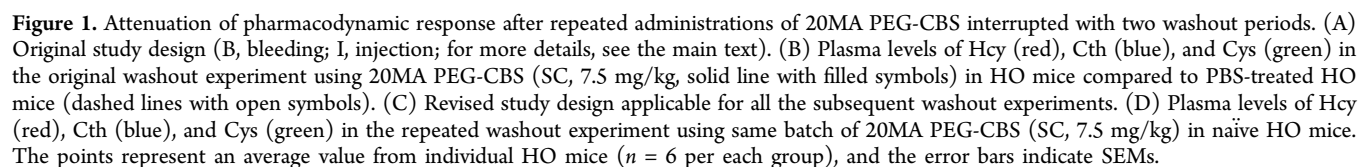
**Nonreduced Capillary Electrophoresis (NR-CE).** Various CBS and PEG-CBS preparations were analyzed on PA800 capillary electrophoresis system (Beckman Coulter, CA, USA) equipped with 30 cm long, 50 µm ID bare-fused silica capillary. The capillary was cut to provide a total length of a 30 cm with a distance of approximately 20 cm from sample introduction inlet to detection window and installed in a cartridge with a 100 × 800 µm aperture. The capillary was preconditioned with 0.1 M NaOH wash followed by 0.1 M HCl wash before it was rinsed with water and final equilibration with SDS MW sample buffer. Protein samples of concentrations less than 10 mg/mL and in a formulation containing high salt were buffer exchanged in water twice (~7-fold dilution each time) to remove matrix interference, diluted to 1 mg/mL final concentration, and denatured by heating at 80 °C for 5 min. Sample was loaded by a high-resolution method using electrokinetic injection (5 kV) for a duration of 20 s and separated for 50 min under voltage of 15 kV. Electropherograms were recorded at a UV wavelength of 220 nm and analyzed using 32karat software (Beckman Coulter, CA, USA).

**Protein Purification and PEGylation.** Human truncated CBS carrying the C15S mutation (htCBS C15S) was expressed and purified as described elsewhere.<sup>11</sup> The purified enzyme was formulated and concentrated using Labscale TFF system (Millipore, MA, USA) equipped with Pellicon XL 50 Ultracel 30 cartridge (regenerated cellulose 30 kDa MWCO membrane) into 200 mM potassium phosphate pH 6.5 or 100 mM sodium phosphate pH 7.2. Activated PEG molecules with either maleimide or NHS ester coupling group characterized by the absence of impurities, such as diols, and narrow molecular weight distributions were purchased from NOF (Japan). PEGylation of htCBS with maleimide and NHS ester PEG was carried out in 100 mM potassium phosphate pH 6.5 and 50 mM sodium phosphate pH 7.2, respectively, by adding PEG dissolved in Milli-Q water in the desired molar ratio (typically CBS subunit/PEG = 1:10) to a final protein concentration of 5 mg/mL. Reaction was carried out at 4 °C overnight. Subsequently, reaction mixture was diluted twice with Milli-Q water, buffer exchanged into Gibco 1× PBS (Thermo Fisher Scientific, MA, USA), and concentrated using Labscale TFF system with Pellicon XL 50 Biomax 100 cartridge (poly(ether sulfone) 100 kDa MWCO membrane). The final PEG-CBS conjugates were filter sterilized (Millipore's 0.2 µm PVDF membrane filter), aliquoted, flash frozen in liquid nitrogen, and stored at –80 °C.

**Protein Gel Electrophoresis.** Protein concentrations were determined by the Bradford assay (Thermo Pierce, MA, USA) using bovine serum albumin (BSA) as a standard according to the manufacturer's recommendations. Denatured proteins were separated by SDS-PAGE using a 10% MiniProtein TGX gels (Biorad, CA, USA), while native samples were resolved by native PAGE in 4–15% Mini-Protein TGX gels. For visualization, the gels were stained with Simple Blue (Invitrogen, CA, USA). Free PEG and PEGylated species were visualized using barium iodide staining as described elsewhere.<sup>18</sup>

**CBS Activity Assay.** The CBS activity was determined by a previously described radioisotope assay using L-[<sup>14</sup>C]-serine as the labeled substrate<sup>11,19</sup> with the following modification. Plasma samples from Alzet pump study were assayed using a modified protocol in a 96-well plate format. Four or five microliters of undiluted plasma was assayed in a total volume of 100 µL for 30 min. The reaction was terminated by mixing of 20 µL of a reaction mixture with 5 µL of chilled performic acid (30% H<sub>2</sub>O<sub>2</sub>/100% formic acid = 1:9) and further processed as described in the original protocol.

**PEGylation Mapping.** Mapping of maleimide and NHS ester PEGylation of htCBS C15S was performed using ESI-QTOF mass spectrometer model 6538 (Agilent, CA, USA). Unmodified enzyme as a control and PEGylated CBS were used as is (unmodified htCBS C15S and 40MA PEG-CBS) or dePEGylated by incubating the sample at pH 11.5 for 22 h at 37 °C (20NHS PEG-CBS). All samples were buffer exchanged, denatured, reduced with 10 mM DTT, and alkylated with 30 mM iodoacetamide prior to digestion. The 40MA PEG-CBS and 20NHS PEG-CBS were digested overnight with Lys-C and Asp-N



LC–UV–MS/MS chromatograms were analyzed using MassHunter software (Agilent, CA, USA). Peptide mapping and sequence matching were performed using BioConfirm package (Agilent, CA, USA) with manual validation to ensure correct assignment.



**Table 1.** Changes in Plasma Sulfur Amino Acid Levels after Treatment of HO Mice with PEGylated htCBS C15S Conjugates<sup>a</sup>

test substance	figure	dose-week W1			dose-week W2			dose-week W3		
		D1 (μM)	D5 (μM)	Δ (%)	D15 (μM)	D19 (μM)	Δ (%)	D29 (μM)	D33 (μM)	Δ (%)
Plasma Total Homocysteine (Hcy)										
20MA PEG-CBS	1B	155 ± 14	56 ± 4	64**	167 ± 15	129 ± 20	23*	n/a	n/a	n/a
PBS (control)	1B	176 ± 19	225 ± 29	−28 <sup>ns</sup>	203 ± 16	189 ± 22	7 <sup>ns</sup>	n/a	n/a	n/a
20MA PEG-CBS	1D	240 ± 26	43 ± 3	82***	242 ± 12	108 ± 17	56***	206 ± 19	119 ± 21	42*
40MA PEG-CBS	2A	134 ± 22	36 ± 4	73**	107 ± 15	53 ± 8	50*	121 ± 16	56 ± 9	54*
40GL4 PEG-CBS	2B	170 ± 14	43 ± 4	75***	159 ± 16	118 ± 16	26 <sup>ns</sup>	161 ± 19	112 ± 21	30 <sup>ns</sup>
40MA PEG-CBS	2C	239 ± 11	60 ± 5	75***	183 ± 11	134 ± 11	27*	237 ± 11	140 ± 10	41***
5NHS PEG-CBS	6A	192 ± 17	48 ± 4	75***	175 ± 17	121 ± 17	31*	201 ± 20	111 ± 7	45**
20NHS PEG-CBS	6B	164 ± 16	38 ± 4	77***	165 ± 20	49 ± 6	70***	142 ± 19	56 ± 10	60***
20MA PEG-CBS	6C	224 ± 14	44 ± 3	80***	215 ± 17	88 ± 11	59**	224 ± 15	112 ± 13	50***
Plasma Cystathionine (Cth)										
20MA PEG-CBS	1B	4.1 ± 0.2	36.3 ± 2.0	796***	4.0 ± 0.3	24.7 ± 3.6	514**	n/a	n/a	n/a
PBS (control)	1B	4.5 ± 0.3	4.5 ± 0.5	−1 <sup>ns</sup>	5.4 ± 0.9	3.7 ± 0.4	−32 <sup>ns</sup>	n/a	n/a	n/a
20MA PEG-CBS	1D	4.8 ± 0.4	31.2 ± 2.2	550***	3.9 ± 0.4	43.1 ± 1.7	1008***	3.9 ± 0.3	20.6 ± 3.8	428**
40MA PEG-CBS	2A	5.0 ± 0.5	24.2 ± 2.4	383***	3.6 ± 0.2	21.5 ± 3.4	494**	3.6 ± 0.4	23.4 ± 4.4	552**
40GL4 PEG-CBS	2B	3.2 ± 0.3	22.1 ± 1.8	588***	3.1 ± 0.4	26.3 ± 7.3	760*	2.7 ± 0.3	17.7 ± 3.2	560**
40MA PEG-CBS	2C	4.1 ± 0.4	29.7 ± 2.1	623***	2.9 ± 0.2	19.7 ± 2.7	591***	3.6 ± 0.5	22.3 ± 3.7	527**
5NHS PEG-CBS	6A	4.0 ± 0.5	42.6 ± 5.3	978***	3.6 ± 0.5	35.4 ± 4.5	887***	4.1 ± 0.4	31.7 ± 3.1	670***
20NHS PEG-CBS	6B	5.0 ± 0.6	37.5 ± 4.5	646***	3.5 ± 0.3	23.3 ± 2.5	565***	4.0 ± 0.4	24.9 ± 2.9	518***
20MA PEG-CBS	6C	3.5 ± 0.3	39.7 ± 1.5	1017***	3.4 ± 0.3	28.8 ± 1.1	737***	3.5 ± 0.5	42.6 ± 3.4	1134***
Plasma Total Cysteine (Cys)										
20MA PEG-CBS	1B	171 ± 8	222 ± 8	30*	163 ± 9	190 ± 12	17*	n/a	n/a	n/a
PBS (control)	1B	166 ± 8	145 ± 13	−13 <sup>ns</sup>	159 ± 11	154 ± 12	−3 <sup>ns</sup>	n/a	n/a	n/a
20MA PEG-CBS	1D	150 ± 7	256 ± 13	71***	116 ± 6	194 ± 13	67***	138 ± 10	197 ± 13	42*
40MA PEG-CBS	2A	184 ± 16	213 ± 10	15 <sup>ns</sup>	150 ± 7	196 ± 8	31*	150 ± 4	198 ± 13	32*
40GL4 PEG-CBS	2B	115 ± 9	227 ± 7	98***	152 ± 14	165 ± 11	8 <sup>ns</sup>	150 ± 11	174 ± 10	16 <sup>ns</sup>
40MA PEG-CBS	2C	123 ± 5	211 ± 7	72***	127 ± 5	177 ± 10	40***	134 ± 3	176 ± 8	31***
5NHS PEG-CBS	6A	129 ± 12	215 ± 10	67***	137 ± 15	192 ± 16	41***	150 ± 18	174 ± 10	16 <sup>ns</sup>
20NHS PEG-CBS	6B	147 ± 10	220 ± 13	49**	149 ± 10	237 ± 6	58***	148 ± 6	222 ± 6	50***
20MA PEG-CBS	6C	124 ± 7	218 ± 11	76***	118 ± 8	205 ± 10	73***	144 ± 13	184 ± 14	28*

<sup>a</sup>The data represent means  $\pm$  SEMs at baseline (i.e., study day D1, D15, and D29) before the first injection of each dose-week W1, W2, and W3 (where applicable; see Figure 1A and C for study designs) and 24 h after the 4th injection in the respective dose-week (i.e., study day D5, D19, and D33). The  $\Delta$  values show the decrease (for Hcy) or increase (for Cth and Cys) of the metabolite plasma levels after four doses for each dose-week compared to the respective baseline in percentages. For each dose-week, the metabolite plasma levels 24 h after the 4th injection were compared to the respective baseline using two-tailed, paired Student's *t*-test to determine significance: \*,  $p < 0.05$ ; \*\*,  $p < 0.01$ ; \*\*\*,  $p < 0.001$ ; ns, non-significant. n/a, not applicable.

**Statistical Analysis.** All data are presented as mean  $\pm$  standard error of the mean (SEM). Statistical assessment of metabolites levels within the same group (e.g., before and after treatment) was conducted using a paired, two-tailed Student's *t* test. Statistical comparison of the two groups were conducted using an unpaired, two-tailed Student's *t* test. Statistical analysis of three or more factor levels was conducted by ANOVA followed by Tukey's multiple comparison test to determine significance. The  $p$  value of less than 0.05 corresponds to statistical significance.

## RESULTS

### Repeated Administration Interrupted with a Washout Period Lead to Attenuation of 20MA PEG-CBS Efficacy.

In our previous study,<sup>11</sup> we assessed multiple PEG-CBS conjugates and concluded that htCBS C15S modified with 20 kDa maleimide PEG (ME-200MA0B) is the most promising candidate to move forward with. To support our decision, we performed a washout study in HO mice. The study design is illustrated in Figure 1A and included subcutaneous injections of 7.5 mg/kg 20MA PEG-CBS for five consecutive days during the first dose-week. Dosing was then interrupted for a period of 10 days and restarted again for an additional five consecutive injections in the second dose-week. Plasma samples were

collected before the very first dose for baseline values, 24 h after the second, fourth, fifth injections in both dose-weeks to track the enzyme's efficacy and during washout periods to follow recovery of the baseline values (a week after the last dose in both dose-weeks, prior to the first dose of the dose-week 2 and 2 weeks after the very last dose). To our surprise, we found out that such study design resulted in an apparent attenuation of 20MA PEG-CBS efficacy in the dose-week 2 compared to dose-week 1 (Figure 1B, Table 1). The attenuated efficacy of 20MA PEG-CBS apparent from the Hcy levels correlated with the lower increase of plasma Cth and Cys in dose-week 2 compared to the first round of injections. Plasma levels of these sulfur amino acids did not significantly vary throughout the study in control HO mice injected with PBS.

To confirm this unexpected result, we repeated the study with the same batch of 20MA PEG-CBS using a new batch of naïve HO mice. Revised study design as shown in Figure 1C included an additional third dose-week, and collection of plasma samples was also slightly adjusted (sample taken 24 h after the last injection of each dose week was replaced with the one taken 72 h post last injection of each dosing period). We

Table 2. CBS Specific Activities of Unmodified htCBS C15S and Various PEG-CBS Conjugates

test substance	PEG moiety	PEG moiety size and structure	PEG active moiety (target group)	CBS specific activity (U/mg of protein $\pm$ SD)	<i>in vivo</i> testing?
htCBS C15S	none	n/a <sup>a</sup>	n/a <sup>a</sup>	1233 $\pm$ 201	no
2MA PEG-CBS	ME-020MA	2 kDa linear	maleimide (-SH)	1184 $\pm$ 95	no
20MA PEG-CBS	ME-200MA0B	20 kDa linear	maleimide (-SH)	1339 $\pm$ 226	yes (Figures 1B,D and 6C)
40MA PEG-CBS	ME-400MA	40 kDa linear	maleimide (-SH)	1242 $\pm$ 158	yes (Figure 2A,C)
40GL4 PEG-CBS	GL4-400MA	40 kDa 4-arm branched	maleimide (-SH)	1288 $\pm$ 221	yes (Figure 2B)
80GL2 PEG-CBS	GL2-800MA	80 kDa 2-arm branched	maleimide (-SH)	1168 $\pm$ 134	no
5NHS PEG-CBS	ME-050GS	5 kDa linear	NHS ester (-NH <sub>2</sub> )	1250 $\pm$ 52	yes (Figure 6A)
10NHS PEG-CBS	ME-100GS	10 kDa linear	NHS ester (-NH <sub>2</sub> )	1233 $\pm$ 173	no
20NHS PEG-CBS	ME-200GS	20 kDa linear	NHS ester (-NH <sub>2</sub> )	1339 $\pm$ 242	yes (Figure 6B)

<sup>a</sup>n/a, not applicable.

reproduced the previously observed attenuation of the 20MA PEG-CBS efficacy (Figure 1D, Table 1).

#### Bulkier Maleimide PEG Did Not Resolve the Attenuation of PEG-CBS Efficacy in the Washout Experiments.

Since the use of maleimide PEG, which specifically targets available sulfhydryl residues, was preferable to yield defined species, our initial approach to tackle the loss of 20MA PEG-CBS efficacy in the washout experiments was to increase the coverage of the htCBS C15S protein with a bulkier maleimide PEG. Our previous data showed that PEGylation of htCBS with larger maleimide PEG did not affect the catalytic activity *in vitro* and that the 40 kDa linear (ME-400MA) or branched (GL4-400MA) maleimide PEG had similar pharmacokinetics (PK) and pharmacodynamics (PD) after a single injection in HO mice compared to 20MA PEG-CBS.<sup>11</sup> In addition, Table 2 shows that the PEGylation of htCBS C15S does not substantially affect the enzyme's catalytic activity regardless of the PEG moiety size and the target group/residue. Thus, we evaluated two additional PEG-CBS conjugates modified with ME-400MA (40MA PEG-CBS) and GL4-400MA (40GL4 PEG-CBS) in a washout experiment (Figure 2, Table 1). The 40MA PEG-CBS showed quite promising profiles of plasma Hcy, Cth, and Cys levels and sustainable efficacy over the course of the study (Figure 2A). On the other hand, the 40GL4 PEG-CBS showed a substantial loss of efficacy in subsequent dose-weeks (Figure 2B). The average initial Hcy levels of HO mice used in 40MA PEG-CBS washout study were somewhat below our cutoff limit: 134 versus 150  $\mu$ M limit. Therefore, we repeated the experiment with a new batch of 40MA PEG-CBS and new set of naïve HO mice with higher basal plasma Hcy. As Figure 2C and Table 1 illustrate, we encountered substantial attenuation of the 40MA PEG-CBS efficacy. These results suggested that the issue of loss of PEG-CBS efficacy could not be solved by an increased molecular size and coverage by a bulkier PEG.

**PEGylation of htCBS C15S with Maleimide PEGs Yielded Inconsistent Results.** While we reported previously<sup>11</sup> that mutating the C15 residue to serine (C15S) would result in uniform PEGylation of htCBS, the conjugation of htCBS C15S with maleimide PEGs still suffered from batch-to-batch variability in this study resulting in heterogeneous PEG-CBS batches (Figure 3). In general, PEGylations with linear 20 and 40 kDa maleimide PEG (20MA and 40MA PEG-CBS batches) resulted in predominant formation of the major (desired) species as shown in Figure 3A. However, the inconsistent presence of residual unmodified htCBS C15S enzyme (Figure 3A) and an irreproducible ratio of individual

PEGylated species as shown on native-PAGE (Figure 3B) represent an important manufacturing challenge. Particularly the presence of unmodified enzyme was problematic as its PK properties are significantly different from PEG-CBS species and may be more immunogenic than the enzyme protected by the PEG envelope.<sup>11,20</sup> We have tried various approaches such as reduction of accessible cysteines with TCEP prior to PEGylation to enhance the yield of the modified enzyme or multiple PEGylation schemes to gain consistency in the process. However, such adjustments only partially improved the consistency of PEGylation (data not shown).

**The 40 kDa Maleimide PEG Modifies Cysteine Residues C272 or C275 in htCBS C15S.** To understand the PEGylation patterns and to optimize the conjugation to yield a more uniform modification, we separated the individual PEG-CBS species and identified the residues targeted with the ME-400MA maleimide PEG (Figure 4). Figure 4A shows the chromatographic separation of 40MA PEG-CBS and the recovery of two pools, which were subsequently analyzed along with an unmodified htCBS C15S and 40MA PEG-CBS reaction mixture on SDS-PAGE (Figure 4B) and native PAGE (Figure 4C). Gel analysis of the pools clearly showed that the 40MA PEG-CBS consisted of at least three different PEG-CBS species. Pool 1 (P1) was enriched in forms, which had a weaker negative charge (Figure 4A) and more PEG moieties attached (Figure 4C) than pool 2 (P2). The predominant PEG-CBS conjugate in P1 consisted of a dimeric htCBS C15S, where each subunit was modified with ME-400MA to the same extent, most likely two PEGs per CBS dimer (*homo*PEGylated dimer). Moreover, P1 contained a minor PEG-CBS species with an additional one or two PEG moieties attached on htCBS C15S dimer. On the other hand, the major PEG-CBS form of P2 contained a dimeric enzyme, where just one of the subunits was modified with PEG, that is, one PEG per CBS dimer (*hemi*PEGylated dimer). Separation of individual PEG-CBS species enabled the identification of the sites of maleimide PEGylation using LC-MS (Figure 4D, see the Supporting Information for details on relative abundance of peptides and estimated number of PEGs per peptide for each particular 40MA PEG-CBS batch). In the phase I, the unmodified htCBS C15S, P1, and P2 were digested with Lys-C. Out of eight cysteine-containing peptides identified from the reduced/alkylated LC-MS peptide map, seven such peptides yielded similar relative abundances in all three samples indicating that these peptides were unlikely to have been PEGylated. Only one peptide (272-322; Figure 4D green highlight) containing two cysteine residues (C272 and C275) showed a significant

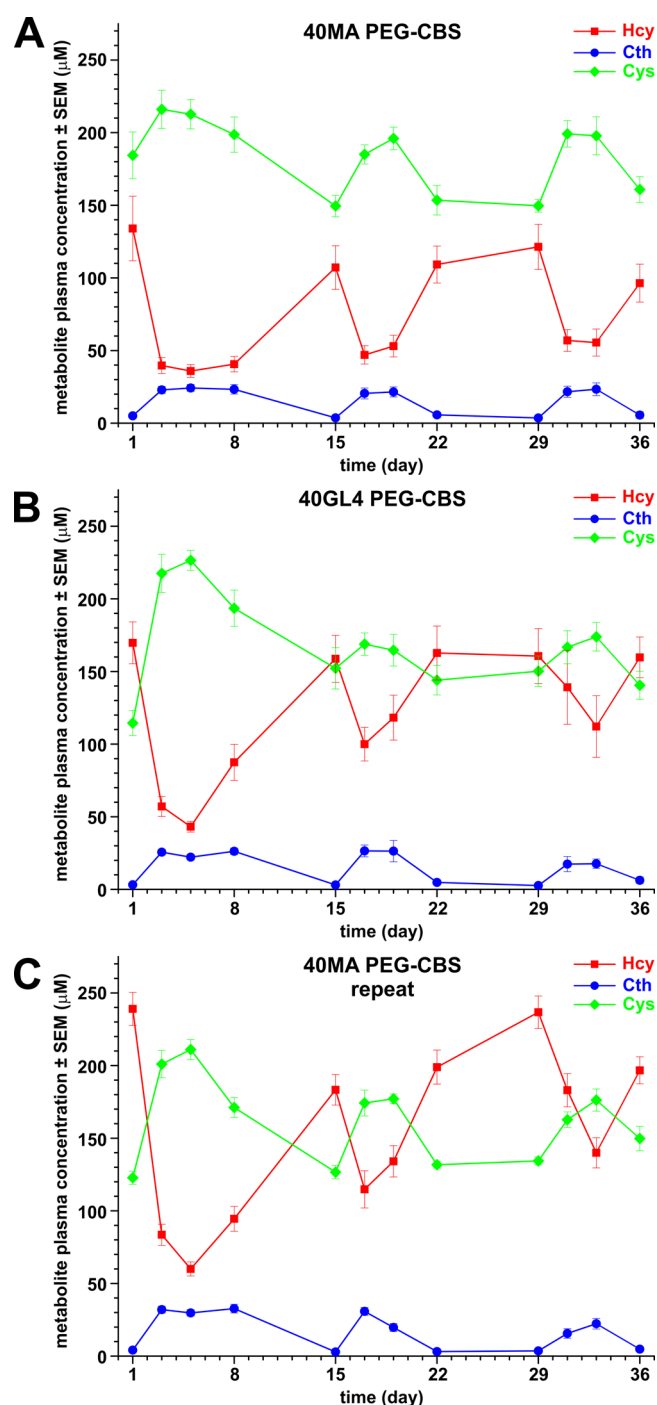


**Figure 2.** Evaluation of additional maleimide PEG-CBS conjugates in a washout experiment. Plasma levels of Hcy (red), Cth (blue), and Cys (green) after repeated administration of (A) 40MA PEG-CBS, (B) 40GL4 PEG-CBS, and (C) of an additional batch of 40MA PEG-CBS in HO mice (SC, 7.5 mg/kg). The experiments followed the revised study design shown in Figure 1C. The points represent an average value from individual HO mice ( $n = 6$ ), and the error bars indicate SEMs.

decrease in each of the two PEG-CBS pools (P1 and P2). In phase II, in an attempt to further differentiate whether C272 or C275 was modified, the two residues would need to be separated into different peptides. Reagent NTCB cleaves N-terminally to a free cysteine residue and only one peptide (244–271; Figure 4D blue highlight) showed a significant

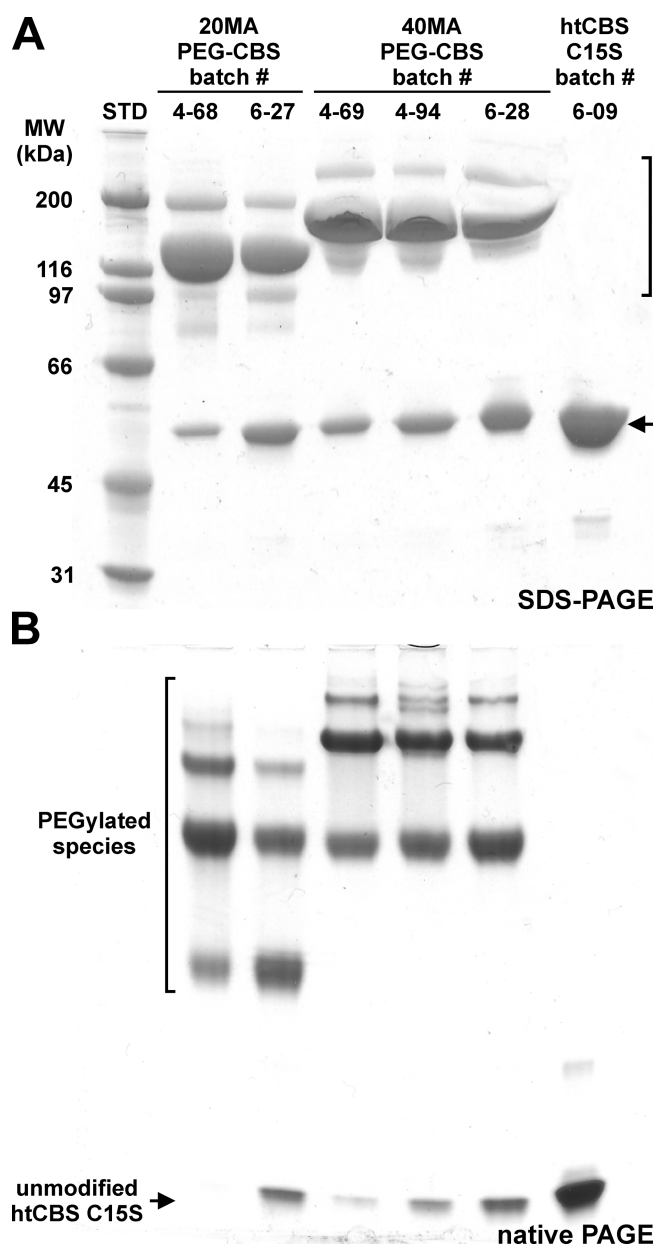


**Figure 3.** Inconsistency in htCBS C15S PEGylation with maleimide PEGs. Linear 20 kDa and 40 kDa maleimide PEGs were used to modify htCBS C15S yielding two 20MA batches (4–68 and 6–27) and three 40MA batches (4–69, 4–94 and 6–28), respectively. Individual PEG-CBS conjugates were buffer-exchanged and formulated into PBS, separated on SDS-PAGE (A, Biorad's 10% Miniprotein TGX gel) or native PAGE (B, Biorad's 4–15% Miniprotein TGX gel) and stained with Safe Stain (Invitrogen) according to manufacturer's recommendation. The arrow points to unmodified htCBS C15S, while the black bracket encompasses the region to which the PEG-CBS conjugates migrated.

decrease in PEG-CBS forms (more in P1 than for P2) compared to similarly treated unmodified htCBS C15S. The lower yield of the 244–271 peptide in PEG-CBS forms signifies that C272 is blocked thus representing the primary site for maleimide PEGylation. It is possible that both cysteine residues C272 and C275 are involved in the PEGylation of higher molecular weight species present in low abundance in P1. Unfortunately, we were unable to draw solid conclusion due to

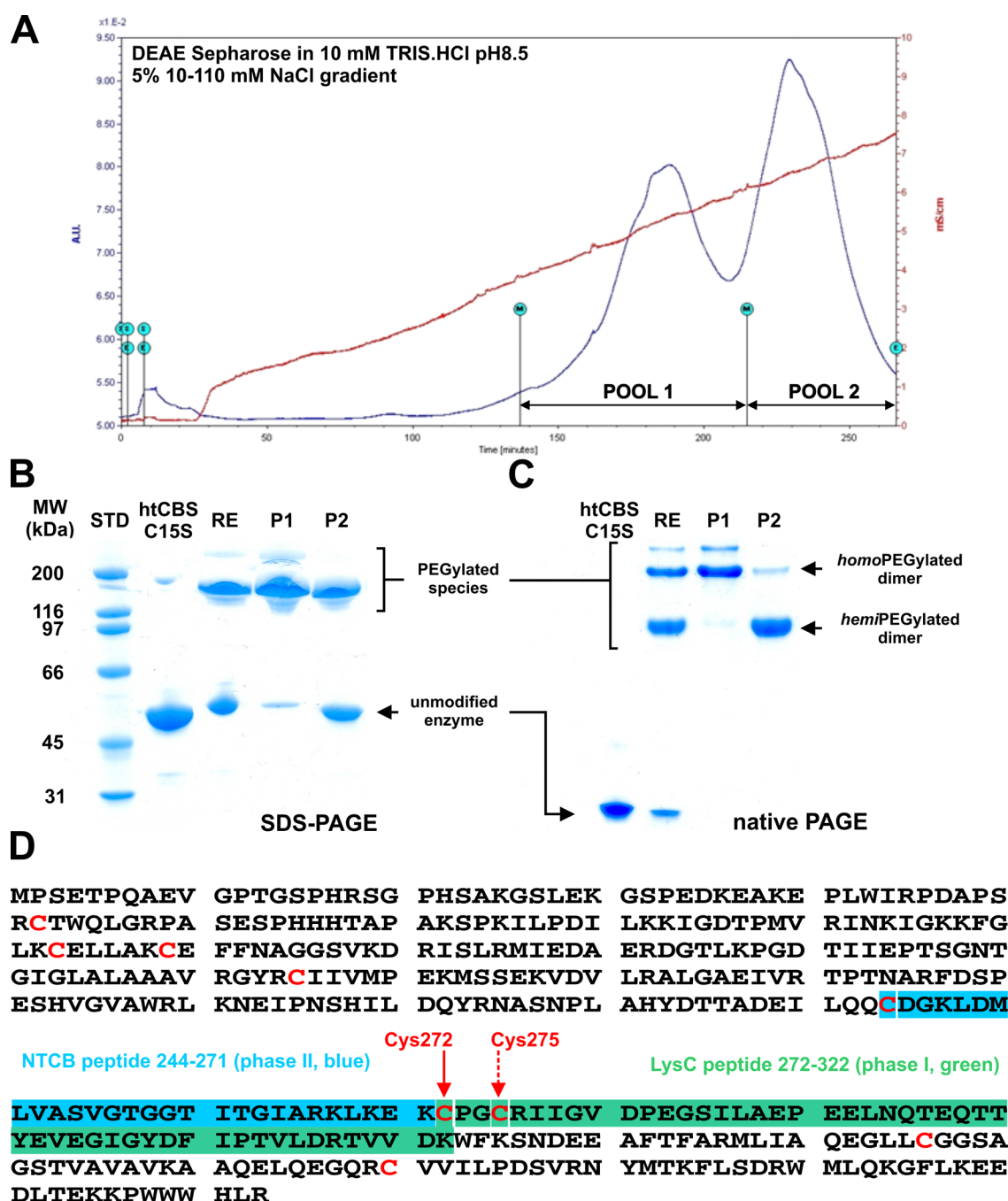


**Figure 4.** Separation of 40MA PEG-CBS species, their characterization, and identification of the PEGylation sites. (A) Chromatographic separation of 40MA PEG-CBS mixture on DEAE Sepharose using shallow salt gradient (5%, 10–110 mM NaCl). The blue trace designates the absorbance at 280 nm, while the red trace designates conductivity of the mobile phase. (B, C) Two recovered pools (P1 and P2) of PEG-CBS species from the chromatographic separation were resolved together with the 40MA PEG-CBS mixture (RE) and the unmodified htCBS C15S on SDS-PAGE (B, Biorad's 10% Miniprotein TGX gel) and native PAGE (C, Biorad's 4–15% Miniprotein TGX gel) and stained with Safe Stain (Invitrogen) according to manufacturer's recommendation. (D) The htCBS C15S protein sequence map showing all cysteine residues (red), Lys-C peptide 272–322 (green highlight), and NTCB peptide 244–271 (blue highlight) showing lower abundance in phase I and II, respectively, of PEGylation site identification using LS-MS compared to their recovery from unmodified htCBS C15S. Solid and dashed red arrows point to C272 as the primary and C275 as the secondary PEGylation site, respectively.

very low NTCB digestion efficiency and too low abundance of the recovered peptides.

**PEGylation of htCBS C15S with NHS Ester PEG Results in a Mixture of Highly Modified Inseparable PEG-CBS Species.** The troublesome reproducibility of htCBS C15S PEGylation with maleimide PEGs prompted us to revisit other PEGylation chemistries we briefly tested earlier,<sup>11</sup> particularly

the use of NHS ester-activated PEGs. First we assessed the modification of htCBS C15S with three NHS ester PEGs and their impact on enzyme activity (Figure 5). Four, three, and two different PEG/CBS molar ratios were tested in PEGylations with 5, 10, and 20 kDa linear NHS ester-activated PEG, respectively. In all cases, the PEGylation yielded a mixture of highly modified PEG-CBS species inseparable by SDS-PAGE



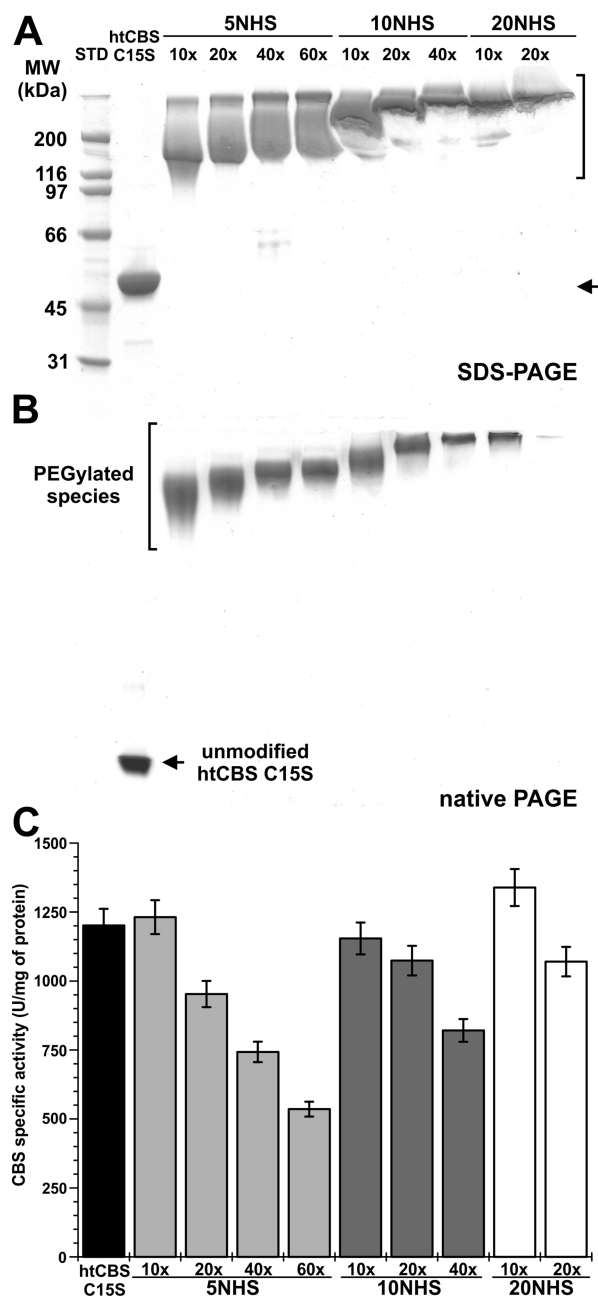


**Figure 5.** PEGylation of C15S htCBS with various NHS ester PEGs. Three linear 5, 10, and 20 kDa NHS ester PEGs (5NHS, 10NHS, and 20NHS) were used to modify htCBS C15S in a variable molar excess of PEG to CBS subunit. Individual PEG-CBS conjugates were separated on SDS-PAGE (A, Biorad's 10% Miniprotean TGX gel) or native PAGE (B, Biorad's 4–15% Miniprotean TGX gel) and stained with Safe Stain (Invitrogen) according to manufacturer's recommendation. The arrow points to unmodified htCBS C15S, while the black bracket encompasses the region where PEG-CBS conjugates migrated. (C) CBS specific activity of various NHS PEG-CBS conjugates compared to unmodified htCBS C15S. Bars represent average from three separate measurements and error bars designates SEMs.

(Figure 5A) as well as by native PAGE (Figure 5B). However, while a 10–20-fold molar excess of PEG to CBS subunit yielded PEG-CBS species with only a slight effect on CBS activity, higher excess of PEG, such as 40- and 60-fold for 5 kDa and 40-fold for 10 kDa NHS PEG resulted in a markedly reduced activity of the respective PEG-CBS conjugates (Figure

5C). Thus, conjugation of htCBS C15S with either NHS PEG in a PEGylation reaction with no more than 20-fold PEG/CBS molar excess yielded highly modified, bulky PEG-CBS conjugates with essentially fully retained activity.

**20NHS PEG-CBS Showed the Smallest Loss of Efficacy in Washout Experiment.** Subsequently, we evaluated two new NHS ester PEG-CBS conjugates modified with 5 kDa ME-050GS (5NHS PEG-CBS) and 20 kDa ME-200GS (20NHS PEG-CBS) in washout experiments and benchmarked them against the current lead candidate 20MA PEG-CBS (Figure 6, Table 1). Similar to maleimide PEG-CBS conjugates, the 5NHS PEG-CBS showed an excellent PD response after the first set of injections with a marked loss of efficacy in the subsequent dose-weeks (Figure 6A, Table 1). In contrast, the 20NHS PEG-CBS showed a significant reduction of Hcy and increase in Cys in the first dose-week, which was sustained in the following dose-weeks (Figure 6B, Table 1). As a control experiment, we analyzed another batch of 20MA PEG-CBS in a washout experiment and again observed attenuated efficacy in subsequent dose-weeks (Figure 6C, Table 1). Taken together, out of all the *in vivo* studied PEG-CBS conjugates, the 20NHS PEG-CBS showed the best PD sustainability after repeated administration of the PEGylated enzyme to HO mice (Figure 6B, Table 1).

**PEGylation of htCBS C15S with 20NHS Ester PEG Showed Good Reproducibility.** Similarly, as we did for the maleimide PEGs, we assessed the reproducibility of htCBS C15S PEGylation with 20NHS PEG. Initial batches suffered from highly variable extent of PEGylation (data not shown). However, we were able to quickly identify the main culprit of such variability being the residual ammonium sulfate in unmodified htCBS C15S. We, therefore, employed an extensive buffer exchange scheme at the end of the chromatographic purification (15–20 diavolumes) to formulate the enzyme into the pre-PEGylation buffer, which resulted in a reproducible PEGylating pattern (Figure 7). The 20NHS PEG-CBS conjugate showed one major high molecular weight band on SDS-PAGE (Figure 7A), which was resolved into a compact smear of highly modified inseparable species on a native PAGE (Figure 7B). Compared to all the previous PEG-CBS conjugates, the 20NHS PEG-CBS showed increased viscosity (determined by using rheometer; data not shown), and thus, there was a concern of sufficient free, unreacted PEG removal during the final (post PEGylation) buffer exchange. Indeed, processing of the initial batches (e.g., batches LAB and 10L in Figure 7C) yielded a large amount of unreacted PEG carried over to the final product. Corrective measures, which included removal of 20% DMSO from the mixture, higher MWCO membrane cartridge for TFF unit (100 versus 30 kDa), three-fold larger surface area and two-fold dilution of the PEGylation mixture prior buffer exchange, all helped to reduce the viscosity and resulted in better clearance of free PEG during the final formulation (e.g., batches TR1 and TR2 in Figure 7C).

**NHS Ester PEG Modifies on Average Five Lysines per htCBS C15S Monomer.** Since SDS or native PAGE failed to resolve individual 20NHS PEG-CBS species, two methods were developed to characterize the extent of htCBS C15S PEGylation with ME-200GS (Figure 8). Comparison of SEC-HPLC chromatograms of individual 20NHS PEG-CBS batches with that of unmodified enzyme (Figure 8A) served for determination of PEGylation kinetics and rapid identification of insufficiently PEGylated batches with their possible rescue by adding more PEG to the reaction mixture (i.e., in-process



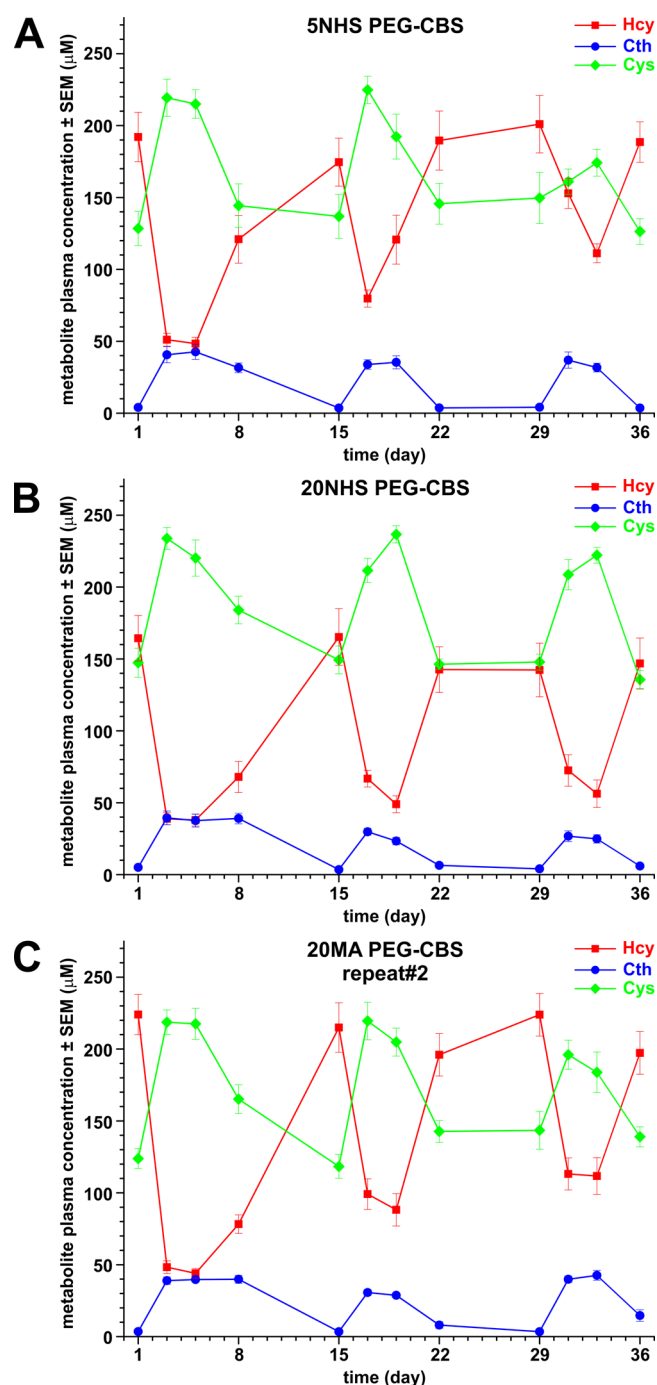


**Figure 6.** Evaluation of NHS ester PEG-CBS conjugates in washout experiments. Plasma levels of Hcy (red), Cth (blue), and Cys (green) after repeated administration of (A) 5NHS PEG-CBS, (B) 20NHS PEG-CBS, and (C) of an additional batch of 20MA PEG-CBS as a benchmarking control in HO mice (SC, 7.5 mg/kg). Experiments followed the revised study design shown in Figure 1C. The points represent an average value from individual HO mice ( $n = 6$ ), and the error bars indicate SEMs.

monitoring of PEGylation). Nonreduced capillary electrophoresis was particularly able to resolve the low molecular weight, insufficiently modified 20NHS PEG-CBS species (Figure 8B), thus making this method suitable for definition of strict and quantifiable acceptance criteria for the drug product.

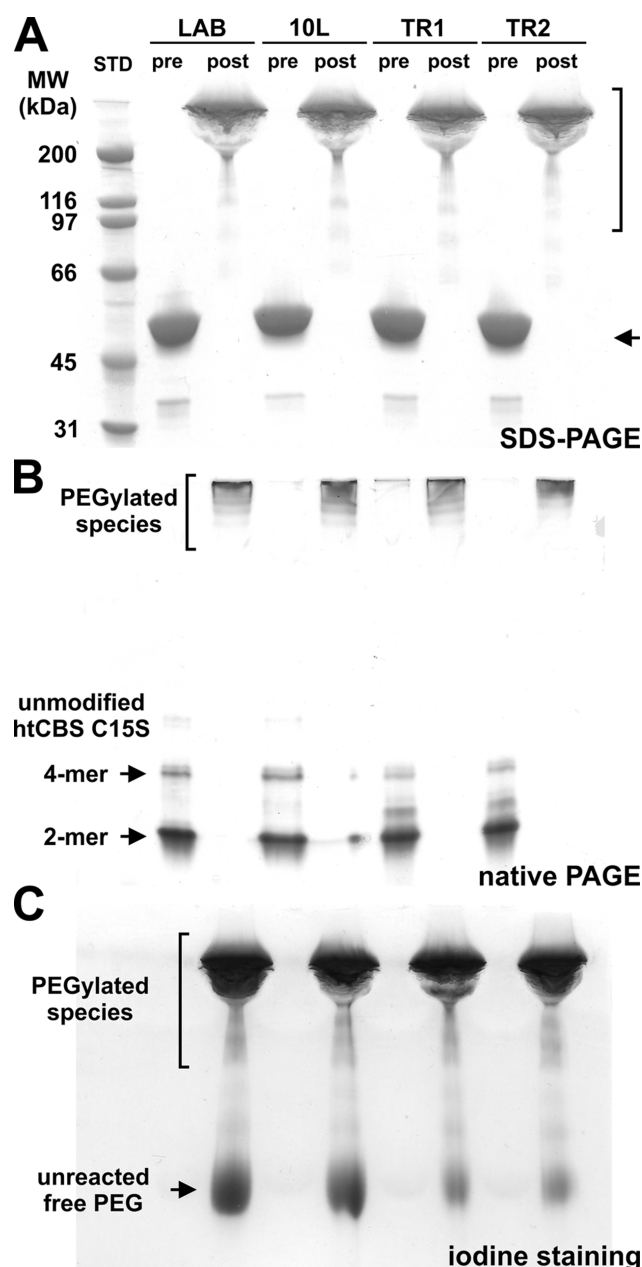


**Figure 7.** PEGylation of htCBS C15S with ME-200GS yielded reproducible batches of 20NHS PEG-CBS. Four batches of purified unmodified htCBS C15S were PEGylated with ME-200GS (10-fold PEG/CBS molar excess) yielding four 20NHS PEG-CBS conjugates. The respective four pairs of unmodified enzyme (pre) and PEG-CBS conjugate (post) were designated as LAB, 10L, TR1, and TR2. The protein samples were resolved in SDS-PAGE (A,C, Biorad's 10% Miniprotein TGX gel) or native PAGE (B, Biorad's 4–15% Miniprotein TGX gel) and stained with (A, B) Safe Stain (Invitrogen) according to manufacturer's recommendation or (C) iodine stained to detect PEG. Arrows in panels A and B point to unmodified htCBS C15S, while the black bracket encompasses the region where PEG-CBS conjugates migrated. Arrow in panel C designates the free unreacted PEG.

The protein sequence of htCBS C15S contains 30 lysine residue. In an attempt to identify the lysine residues involved in NHS ester PEGylation, we performed LC–UV–MS peptide mapping of three 20NHS PEG-CBS batches (Figure 8C). After de-PEGylation, the formerly PEGylated lysines were left with a

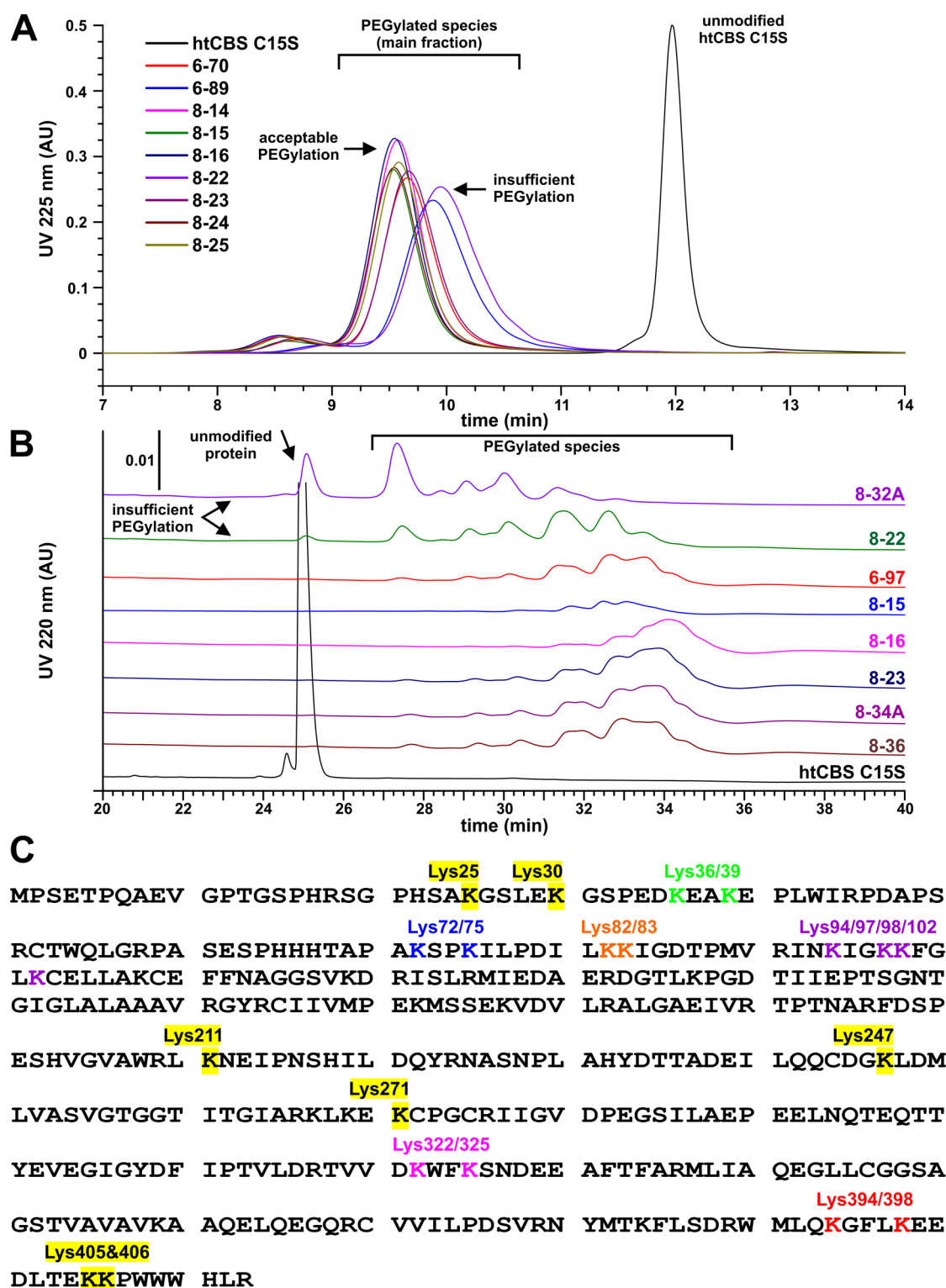


**Figure 8.** Characterization of 20NHS PEG-CBS. (A) SEC-HPLC chromatograms and (B) NR CE profiles of multiple 20NHS PEG-CBS batches compared to unmodified htCBS C15S. (C) htCBS C15S protein sequence map containing 30 lysine residues and summarizing the results from LC–UV–MS peptide mapping. Yellow color highlights residues, which were unequivocally found PEGylated on the respective Asp-N peptides to a certain extent. Green, blue, orange, purple, pink, and red color indicate one of the lysines of the same color on that Asp-N peptide identified as PEGylated at a certain extent (for the exact extent of PEGylation, please see the [Supporting Information](#)).

linker, thus enabling their differentiation from unmodified lysines and quantification via peptide mapping after cleavage with Asp-N endopeptidase and comparison to similarly processed unmodified htCBS C15S. Seven lysines (K25, K30,

K211, K247, K271, K405, and K406) were unambiguously identified as being PEGylated to a certain extent, out of which K25 and K30 residues seemed the only ones to be always modified to the full extent (see the [Supporting Information](#) for

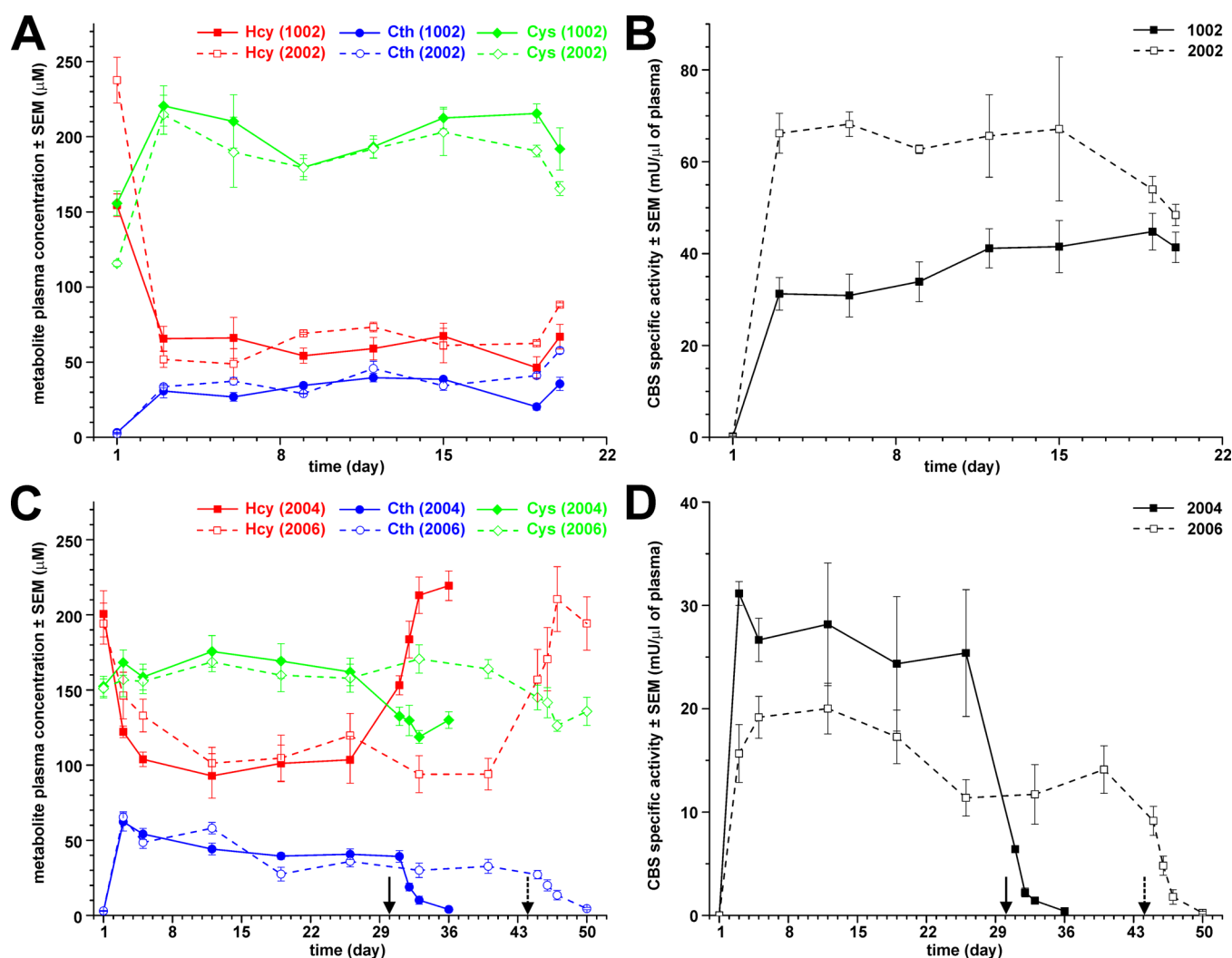


**Figure 9.** Continuous administration of 20NHS PEG-CBS using osmotic pumps. (A) Plasma metabolites and (B) CBS activity for osmotic pumps models 1002 and 2002 without surgical removal intended to deliver 0.25 and 0.5  $\mu\text{L}/\text{h}$ , respectively, of the enzyme for a period of 14 days. Solid lines represent model 1002, while the dashed lines denote model 2002. Red, blue, and green color designate plasma Hcy, Cth, and Cys, respectively. (C) Plasma metabolites and (D) CBS activity for osmotic pumps models 2004 and 2006. The pump model 2004 designed to deliver 0.25  $\mu\text{L}/\text{h}$  of the enzyme for a period of 4 weeks was surgically explanted on day 30, while the pump model 2006 designed to deliver 0.15  $\mu\text{L}/\text{h}$  of the enzyme for a period of 6 weeks was surgically removed on day 44 (explant day designed by solid and dashed arrow for models 2004 and 2006, respectively). Solid lines represent model 2004, while dashed lines denote model 2006. Red, blue, and green color symbolize plasma Hcy, Cth, and Cys, respectively.

details on relative abundance of peptides and estimated number of PEGs per peptide for each particular 20NHS PEG-CBS batch). Further, we identified five and one peptide(s) each harboring two or four lysines, respectively, of which one lysine residue was found inconsistently PEGylated: K36/39, K72/75, K82/83, K94/97/98/102, K322/325, and K394/398. Overall, the extent of PEGylation was estimated to be in the range of  $5.0 \pm 0.5$  PEGs per CBS monomer.

**20NHS PEG-CBS Showed Sustained PD Efficacy and Maintenance of Plasma Levels during Continuous Delivery via Osmotic Pumps.** To complement the washout experiment, we performed an additional *in vivo* study using osmotic pumps designed for steady and continuous delivery of the drug to demonstrate a long-term efficacy of the 20NHS PEG-CBS in HO mice. We utilized four different sizes of the pumps designed to deliver 0.15 to 0.5  $\mu\text{L}/\text{h}$  for a period of 2–6 weeks, thus allowing us to study the dose effect over time (Figure 9, Table 3). Subcutaneously implanted osmotic pump models 1002 (0.25  $\mu\text{L}/\text{h}$  for 14 days) and 2002 (0.5  $\mu\text{L}/\text{h}$  for

14 days) substantially and significantly reduced Hcy, increased Cth, and normalized Cys plasma levels (Figure 9A, Table 3). The effect was sustained well over the intended period of 2 weeks and comparable to that achieved by daily consecutive injections in the washout study (Figure 6B). Metabolic correction was sustained by CBS specific activities of 31–45 and 54–68 mU/ $\mu\text{L}$  of plasma for model 1002 and 2002, respectively (Figure 9B, Table 3).

Since the data showed that doubling the amount of the 20NHS PEG-CBS resulted in similar PD, we evaluated the osmotic pump intended to deliver the same or smaller amounts of the enzyme over a longer period of time. Subcutaneously implanted osmotic pump models 2004 (0.25  $\mu\text{L}/\text{h}$  for 28 days) and 2006 (0.15  $\mu\text{L}/\text{h}$  for 42 days) substantially and significantly reduced plasma Hcy (Figure 9C, Table 3), which was sustained until the pumps were surgically explanted from the mice on day 30 and 44, respectively. However, the achieved Hcy levels were approximately two-fold higher compared to those observed in the previous experiment (Figure 9A, Table 3). Interestingly, the



**Table 3. Plasma Levels of Sulfur Amino Acids and CBS Specific Activities during Continuous Administration of 20NHS PEG-CBS via Subcutaneously Implanted Osmotic Pumps in HO Mice<sup>a</sup>**

osmotic pump	figure	baseline	initial		steady state		
		D1	D3	$\Delta$ (%)	D19	$\Delta$ (%)	$\Delta\Delta$ (%)
Plasma Total Homocysteine (Hcy, $\mu\text{M} \pm \text{SEM}$ )							
1002	9A	155 $\pm$ 8	66 $\pm$ 8	58***	46 $\pm$ 7	70***	29*
2002	9A	238 $\pm$ 15	52 $\pm$ 5	78*	63 $\pm$ 1	74***	−21 <sup>ns</sup>
2004	9C	201 $\pm$ 15	122 $\pm$ 4	39*	101 $\pm$ 12	50**	17 <sup>ns</sup>
2006	9C	194 $\pm$ 14	146 $\pm$ 16	25*	105 $\pm$ 15	46***	28 <sup>ns</sup>
Plasma Cystathionine (Cth, $\mu\text{M} \pm \text{SEM}$ )							
1002	9A	3.2 $\pm$ 0.1	30.8 $\pm$ 4.5	862**	20.3 $\pm$ 2.2	534***	−34*
2002	9A	2.4 $\pm$ 0.4	33.6 $\pm$ 0.7	1312***	41.1 $\pm$ 1.6	1625***	22 <sup>ns</sup>
2004	9C	2.8 $\pm$ 0.2	62.2 $\pm$ 6.0	2097***	39.5 $\pm$ 2.1	1294***	−37*
2006	9C	3.0 $\pm$ 0.3	65.3 $\pm$ 3.7	2073***	27.4 $\pm$ 4.6	813**	−58***
Plasma Total Cysteine (Cys, $\mu\text{M} \pm \text{SEM}$ )							
1002	9A	156 $\pm$ 8	221 $\pm$ 13	42**	216 $\pm$ 6	38***	−2 <sup>ns</sup>
2002	9A	116 $\pm$ 2	215 $\pm$ 13	86*	191 $\pm$ 4	65***	−11 <sup>ns</sup>
2004	9C	152 $\pm$ 7	168 $\pm$ 8	10 <sup>ns</sup>	169 $\pm$ 12	11 <sup>ns</sup>	1 <sup>ns</sup>
2006	9C	151 $\pm$ 6	157 $\pm$ 11	4 <sup>ns</sup>	160 $\pm$ 11	6 <sup>ns</sup>	2 <sup>ns</sup>
Plasma 20NHS PEG-CBS Specific Activity (mU/ $\mu\text{L}$ of plasma)							
1002	9B	0	31 $\pm$ 4	n/a	45 $\pm$ 4	n/a	43*
2002	9B	0	66 $\pm$ 4	n/a	54 $\pm$ 3	n/a	−18 <sup>ns</sup>
2004	9D	0	31 $\pm$ 1	n/a	24 $\pm$ 7	n/a	−22 <sup>ns</sup>
2006	9D	0	16 $\pm$ 3	n/a	17 $\pm$ 3	n/a	10 <sup>ns</sup>

<sup>a</sup>Metabolite concentrations and CBS specific activities in plasma are shown before the osmotic pump implantation (baseline, D1), 3 days after implantation (initial, D3), and at steady state (D19). The  $\Delta$  values show the decrease (for Hcy) or increase (for Cth, Cys, and CBS specific activity) at D3 or D19 compared to D1, while  $\Delta\Delta$  value designate the difference in plasma levels between D19 and D3 in percentages. For each pump type, the data were compared using two-tailed, paired Student's t-test to determine significance: \*,  $p < 0.05$ ; \*\*,  $p < 0.01$ ; \*\*\*,  $p < 0.001$ ; ns, non-significant. n/a, not applicable. For more details, see the main text and Figure 9.

initial Cth levels (D3) were higher, but in general similar to those seen in previously tested pumps. On the contrary, the Cys levels remained similar to baseline levels. The corresponding CBS specific activities were 24–31 and 11–20 mU/ $\mu\text{L}$  of plasma for model 2004 and 2006, respectively (Figure 9D, Table 3). Taken together, the data suggest that these plasma levels of CBS activity are not sufficient to achieve maximal PD efficacy. The removal of the pump in survival surgery resulted in regeneration of the basal Hcy levels, gradual clearance of 20NHS PEG-CBS and Cth from plasma, and, interestingly, marked decrease of Cys below baseline levels (Figure 9C,D). In summary, the substantially lower plasma CBS specific activities (up to 6-fold difference between pump model 2002 shown in Figure 9B and 2006 shown in Figure 9D) resulted in a significant correction of plasma Hcy levels and their maintenance over a period of several weeks without Cys normalization.

## DISCUSSION

An integral part of any novel therapeutic development effort, whether it is a small molecule drug or a biologic, is a selection, optimization, and characterization of the lead candidate to enter the clinical trials. In this study, we described such a process in the quest for an ERT for HCU. Although effective, a treatment of HCU through dietary restrictions to reduce methionine intake is very difficult to follow and suffers from serious patient compliancy issues.<sup>10</sup> The unifying goal of a restricted diet, pyridoxine treatment, or betaine supplementation as the currently available therapeutic options for HCU is to reduce or normalize plasma Hcy levels as fluctuations and high levels are often associated with serious complications, particularly thromboembolic events.<sup>21</sup> Development of an alternative, such

as ERT, would reduce reliance on the dietary restriction or ideally remove it entirely, which in turn would allow HCU patients and their families access to a better quality of life. To achieve this therapeutic goal (i.e., the reduction or normalization of plasma Hcy), we modified the C15S variant of htCBS with a 20 kDa linear maleimide-activated PEG and provided a proof of concept using murine models of homocystinuria.<sup>11</sup>

There is a trend in PEGylation of therapeutic macromolecules from heterogeneous mixtures of conjugate isomers ideally toward a single modified form for obvious reasons, such as characterization/identification of the product and reproducibility of the manufacturing process.<sup>22</sup> Modification of accessible cysteine residue using maleimide PEG represents one of the most commonly used approaches for site selective PEGylation. Despite the mutagenesis of the most accessible cysteine residue 15 into serine (C15S) in htCBS,<sup>23</sup> we still observed multiple PEGylated species in addition to a fraction of an unmodified enzyme using maleimide PEG. Although the individual species were chromatographically separable, such operation would certainly result in substantial losses and would likely render the process prohibitively expensive. The maleimide PEGylation of htCBS C15S was mapped to a peptide containing residues C272 and C275 with former residue being a primary site for modification. Mutagenesis of either cysteine residue would most likely increased reproducibility of PEGylation; however, substantial reduction in heme saturation and catalytic activity was anticipated.<sup>24</sup> In addition to manufacturing issues, both the 20MA and 40MA PEG-CBS conjugates showed reduction in efficacy in HO mice in dose weeks 2 and 3 interrupted with a 10-day washout periods (Figures 1 and 2, Table 1). Such dosing regimen was specifically designed to elicit immune response to rank

candidates based on their immunogenic properties. We have shown previously that the repeated uninterrupted dosing of 20MA PEG-CBS to homocystinuric HO mice resulted in a retained efficacy and a significant decrease of plasma Hcy levels 24 h after injection for a period of 2 months,<sup>11</sup> although both the baseline level (72 h post injection) of plasma Hcy and the peak effect of 20MA PEG-CBS (24 h post injection) were decreasing over time. Although we have not determined it in either of the above-mentioned experiments, the most reasonable explanation for such attenuation of activity is the host's immune response, which may adversely impact both the efficacy and the safety and is relatively common among approved therapeutic enzymes.<sup>25</sup> Alternatively, loss of maleimide PEGylation via retro-Michael addition *in vivo* due to maleimide exchange with reactive thiols in albumin, cysteine, and glutathione might result in a decrease of maleimide PEG-CBS efficacy.<sup>26</sup> However, we have not observed such de-PEGylation in our previous study.<sup>11</sup>

The assumed immunogenicity could stem from either the trace amounts of unmodified enzyme or insufficiently masked htCBS C15S with site selective maleimide PEG conjugation. Therefore, a complete absence of unmodified enzyme and more generous masking of potential immunogenic epitopes of PEG-CBS conjugate from the immune system by increased PEGylation would be expected to prevent the decrease in efficacy. Indeed, when we modified the htCBS C15S enzyme with the 20 kDa NHS ester PEG (ME-200GS) targeting primarily the lysine residues, the 20NHS PEG-CBS conjugate injected to HO mice resulted in the smallest attenuation in efficacy in dose weeks 2 and 3 after the washout periods (Figure 6B). PEGylation of htCBS C15S with lysine-targeting 5, 10, or 20 kDa NHS ester PEGs used in up to a 20-fold molar excess to htCBS C15S subunit did not significantly affect the enzyme's specific activity (Figure 5C), a property shared with the maleimide PEGs.<sup>11</sup> However, unlike the site selective maleimide PEGylation, the NHS ester PEGs yielded a reproducible mixture of highly modified isomers practically inseparable using gel electrophoresis (Figures 5A,B and 7) or SEC-HPLC (Figure 8A). Partial separation was achieved only using NR-CE (Figure 8B), which could serve as a method for "fingerprinting" of the 20NHS PEG-CBS production batches. Similar strategy for PEGylation was employed in the development of an ERT for phenylketonuria based on phenylalanine ammonia-lyase (PAL). Unlike CBS used in our ERT, the PAL is a tetrameric nonmammalian enzyme originating from cyanobacterial and fungal species.<sup>27</sup> Therefore, immunogenicity of such foreign protein represented a substantial concern, and various PEGylation protocols were tested with PAL.<sup>28</sup> The PEG-PAL was conjugated with NHS ester PEGs ranging from a linear 5 kDa up to a branched 40 kDa in size with linear 20 kDa PEG-PAL conjugates demonstrating increased performance and masking immunogenicity the best. Reduction of the PEG-PAL immunogenicity was directly proportional to a number of PEGs attached to the PAL subunit with gel-based estimate of 6–8 PEGs per PAL monomer suppressing the immune response most efficiently.<sup>28</sup> Since PEGs are notorious for not migrating according to their molecular weight in gels or chromatographic applications due to a significant solvation envelope and thus increased hydrodynamic radius,<sup>29</sup> we estimated an average PEGylation of htCBS C15S with the 20 kDa NHS ester PEG to be  $5.0 \pm 0.5$  PEGs/subunit using mass spectrometry (Figure 8C).

More importantly, the 20NHS PEG-CBS showed a sustained PD effect on plasma metabolites and maintained steady plasma levels of enzymatic activity in homocystinuric HO mice when continuously released to an SC compartment from the osmotic pumps for a period of up to 44 days (Figure 9B). Interestingly, continuous release of 20NHS PEG-CBS yielding plasma CBS specific activities from 11 to 67 mU/ $\mu$ L of plasma resulted in significant and substantial drop of plasma Hcy by 50 to 80%, respectively. However, normalization of plasma Hcy concentrations was not observed. For illustration, when PEG-PAL was administered to the PKU mouse model, plasma phenylalanine levels were brought down to zero in a short-term study and after overcoming an initial immune response also in a long-term study.<sup>27</sup> To address this enigma, the Hcy metabolisms and pathophysiology need to be taken into account. Unlike phenylalanine, Hcy is a redox-active thiol group-containing molecule that exists in plasma in a variety of chemical forms (as fractions of total Hcy pool): thiolactone (<1%), free reduced (~2%), disulfide (~18%), and protein-bound (~80%).<sup>30–32</sup> Free Hcy is increased substantially to a 10–25% of total plasma Hcy in homocystinuria.<sup>33</sup> In addition, Hcy in homocystinuria entirely replaces Cys bound to plasma albumin,<sup>34</sup> which may contribute to decreased levels of plasma Cys found in HCU. Albumin is synthesized exclusively in the liver, and its plasma concentration of 33–52 g/L in healthy human represents only ~40%, while the remaining ~60% of albumin stays in extravascular space.<sup>35</sup> In theory, only a free Hcy represents a substrate for CBS. Thus, the 50–80% decrease of total Hcy in HO mice upon continuous administration of 20NHS PEG-CBS could be explained only by shifting the balance in favor of free Hcy compared to other forms (disulfides and protein-bound).<sup>11</sup> Although 20NHS PEG-CBS in circulation serves as a "sink" for excess of Hcy, it may not be enough to normalize the Hcy plasma levels. Possible reasons could be the constant flux of intracellular Hcy (particularly from liver as protein-bound Hcy to a newly synthesized albumin), dynamic balance between intra- and extra-vascular Hcy pools (mediated again mostly via albumin), and homocystinuria-induced pro-oxidative environment favoring disulfides and protein-bound forms of total Hcy pool. Nevertheless, recently published guidelines for diagnosis and management of HCU recommend keeping the plasma total Hcy below 100  $\mu$ M to prevent progress or occurrence of serious complications.<sup>21</sup> If we extrapolate our results on homocystinuric HO mice fed with standard unrestricted chow containing 4–5 g methionine per kg of diet (corresponds to 18–19% of protein), administration of 20NHS PEG-CBS to human HCU patients should result in guidelines-recommended plasma total Hcy levels without any additional treatment. However, ERT is not a trivial procedure and has its own set of limitations.<sup>36</sup> Nevertheless, the data presented in this study show steady progress toward development of ERT for HCU and as such should be a cause for joy for HCU patients and their families struggling with severely protein restricted dietary regimen and betaine supplementation.

## CONCLUSIONS

Development of a new therapeutic often requires screening through multiple compounds, selection of a few candidates, and thorough characterization of lead compound(s) both *in vitro* and *in vivo* prior to initial testing in humans. Here, we showed such a process using PEG-CBS as an enzyme replacement therapy for homocystinuria. We found that modifications of the enzyme with maleimide PEGs yielded inconsistent results with

insufficiently masked conjugates, which resulted in attenuation of potency of the respective PEG-CBS conjugates when repeatedly administered to homocystinuric mice. On the other hand, the enzyme modified with 20 kDa NHS-PEG showed reproducible modification and, more importantly, sustained potency *in vivo*. While maleimide PEG-CBS conjugates were primarily modified at the C272 residue, 20NHS PEG-CBS was extensively masked on average with five PEG chains residues per subunit attached to multiple lysines across the entire protein sequence. The developed SEC-HPLC and NR-CE assays were able to differentiate acceptably from insufficiently modified 20NHS PEG-CBS batches. The 20NHS PEG-CBS further showed a sustained partial normalization of plasma sulfur amino acids in homocystinuric mice upon continuous administration using subcutaneously implanted osmotic pumps. Thus, the 20NHS PEG-CBS conjugate represents the most suitable candidate for manufacturing and clinical development. On the basis of the work reported here, a GLP-tox study using 20NHS PEG-CBS as an ERT for HCU has been initiated to move to a Phase I clinical trial in the near future.

## ■ ASSOCIATED CONTENT

### ■ Supporting Information

The Supporting Information is available free of charge on the ACS Publications website at DOI: 10.1021/acs.biomac.7b00154.

Tables and figures showing results from mass spectrometric characterization of 40MA and 20NHS PEG-CBS conjugates (PDF)

## ■ AUTHOR INFORMATION

### Corresponding Authors

\*E-mail: tomas.majtan@ucdenver.edu. Phone: 303-724-3813. Fax: 303-724-3838.

\*E-mail: jan.kraus@ucdenver.edu. Phone: 303-724-3812. Fax: 303-724-3838.

### ORCID

Tomas Majtan: 0000-0002-2751-2124

### Author Contributions

T.M. designed and performed all the studies, prepared and analyzed PEG-CBS conjugates, analyzed data, wrote the initial draft, revised the manuscript, and approved its final version. I.P. took care of the animal colony, executed animal studies, and approved the final version of the manuscript. R.S.C. prepared the studied PEG-CBS conjugates and approved the final version of the manuscript. E.M.B. co-designed the studies, coordinated collaborations and approved the final version of the manuscript. J.P.K. conceived the idea, designed the studies, revised the manuscript, and approved its final form.

### Notes

The authors declare the following competing financial interest(s): The research was funded by Orphan Technologies Ltd., a private pharmaceutical company developing an enzyme replacement therapy for CBS-deficient homocystinuria. T.M. and J.P.K. are inventors on patents related to the processes and products referred in the manuscript (US patents 9,034,318 and 9,243,239).

## ■ ACKNOWLEDGMENTS

The authors would like to acknowledge Richard Carrillo for htCBS C15S purifications and assistance in preparation of the various PEG-CBS conjugates and Carla Ray, Linda Farb, Sally Stabler, and Robert Allen for determination of plasma sulfur amino acid metabolites. In addition, we would like to thank Rajendrakumar Gosavi and Cale Halbleib from KBI Biopharma for NR-CE runs, Ian Parson and Andrew Hanneman from Charles River Laboratories (formerly Blue Stream Laboratories) for PEGylation mapping, and Carol Nelson from Translational Pharmacology Consulting for assistance with animal data analysis. T.M. is a recipient of the American Heart Association Scientist Development Grant (16SDG30040000). This work was supported by a research grant from Orphan Technologies Ltd. (to J.P.K.). Shared resources of the Colorado Clinical & Translational Sciences Institute (CCTSI), funded in part by Colorado CTSA Grant No. UL1 TR001082 from NCATS/NIH, were used.

## ■ REFERENCES

- (1) Finkelstein, J. D. Methionine metabolism in mammals. *J. Nutr. Biochem.* **1990**, *1*, 228–237.
- (2) Majtan, T.; Pey, A. L.; Ereno-Orbea, J.; Martinez-Cruz, L. A.; Kraus, J. P. Targeting Cystathionine Beta-Synthase Misfolding in Homocystinuria by Small Ligands: State of the Art and Future Directions. *Curr. Drug Targets* **2016**, *17* (13), 1455–1470.
- (3) Ereno-Orbea, J.; Majtan, T.; Oyenarte, I.; Kraus, J. P.; Martinez-Cruz, L. A. Structural insight into the molecular mechanism of allosteric activation of human cystathionine beta-synthase by S-adenosylmethionine. *Proc. Natl. Acad. Sci. U. S. A.* **2014**, *111* (37), E3845–52.
- (4) Kery, V.; Poneleit, L.; Kraus, J. P. Trypsin cleavage of human cystathionine beta-synthase into an evolutionarily conserved active core: structural and functional consequences. *Arch. Biochem. Biophys.* **1998**, *355* (2), 222–32.
- (5) Majtan, T.; Pey, A. L.; Fernandez, R.; Fernandez, J. A.; Martinez-Cruz, L. A.; Kraus, J. P. Domain organization, catalysis and regulation of eukaryotic cystathionine beta-synthases. *PLoS One* **2014**, *9* (8), e105290.
- (6) Mudd, S. H.; Levy, H. L.; Kraus, J. P. Disorders of trans-sulfuration. In *The Metabolic and Molecular Bases of Inherited Disease*, 8th ed.; Scriver, C. R., Beaudet, A. L., Sly, W. S., Valle, D., Childs, B., Kinzler, K., Vogelstein, B., Eds.; McGraw-Hill: New York, 2001; pp 2007–2056.
- (7) Komrower, G. M.; Lambert, A. M.; Cusworth, D. C.; Westall, R. G. Dietary treatment of homocystinuria. *Arch. Dis. Child.* **1966**, *41* (220), 666–71.
- (8) Olthof, M. R.; Verhoeve, P. Effects of betaine intake on plasma homocysteine concentrations and consequences for health. *Curr. Drug Metab.* **2005**, *6* (1), 15–22.
- (9) Clayton, P. T. B6-responsive disorders: a model of vitamin dependency. *J. Inherited Metab. Dis.* **2006**, *29* (2–3), 317–26.
- (10) Walter, J. H.; Wraith, J. E.; White, F. J.; Bridge, C.; Till, J. Strategies for the treatment of cystathionine  $\beta$ -synthase deficiency: the experience of the Willink Biochemical Genetics Unit over the past 30 years. *Eur. J. Pediatr.* **1998**, *157* (S2), S71–S76.
- (11) Bublil, E. M.; Majtan, T.; Park, I.; Carrillo, R. S.; Hulkova, H.; Krijt, J.; Kozich, V.; Kraus, J. P. Enzyme replacement with PEGylated cystathionine beta-synthase ameliorates homocystinuria in murine model. *J. Clin. Invest.* **2016**, *126* (6), 2372–84.
- (12) Fishburn, C. S. The pharmacology of PEGylation: balancing PD with PK to generate novel therapeutics. *J. Pharm. Sci.* **2008**, *97* (10), 4167–83.
- (13) Kolate, A.; Baradia, D.; Patil, S.; Vhora, I.; Kore, G.; Misra, A. PEG - a versatile conjugating ligand for drugs and drug delivery systems. *J. Controlled Release* **2014**, *192*, 67–81.



- (14) Turecek, P. L.; Bossard, M. J.; Schoetens, F.; Ivens, I. A. PEGylation of Biopharmaceuticals: A Review of Chemistry and Nonclinical Safety Information of Approved Drugs. *J. Pharm. Sci.* **2016**, *105* (2), 460–75.
- (15) Maclean, K. N.; Sikora, J.; Kozich, V.; Jiang, H.; Greiner, L. S.; Kraus, E.; Krijt, J.; Overdier, K. H.; Collard, R.; Brodsky, G. L.; Meltesen, L.; Crnic, L. S.; Allen, R. H.; Stabler, S. P.; Elleder, M.; Rozen, R.; Patterson, D.; Kraus, J. P. A novel transgenic mouse model of CBS-deficient homocystinuria does not incur hepatic steatosis or fibrosis and exhibits a hypercoagulable phenotype that is ameliorated by betaine treatment. *Mol. Genet. Metab.* **2010**, *101* (2–3), 153–62.
- (16) Watanabe, M.; Osada, J.; Aratani, Y.; Kluckman, K.; Reddick, R.; Malinow, M. R.; Maeda, N. Mice deficient in cystathionine  $\beta$ -synthase: Animal models for mild and severe homocyst(e)inemia. *Proc. Natl. Acad. Sci. U. S. A.* **1995**, *92*, 1585–1589.
- (17) Allen, R. H.; Stabler, S. P.; Lindenbaum, J. Serum betaine, *N,N*-dimethylglycine and *N*-methylglycine levels in patients with cobalamin and folate deficiency and related inborn errors of metabolism. *Metab. Clin. Exp.* **1993**, *42*, 1448–1460.
- (18) Kurfurst, M. M. Detection and molecular weight determination of polyethylene glycol-modified hirudin by staining after sodium dodecyl sulfate-polyacrylamide gel electrophoresis. *Anal. Biochem.* **1992**, *200* (2), 244–8.
- (19) Kraus, J. P. Cystathionine beta-synthase (human). *Methods Enzymol.* **1987**, *143*, 388–94.
- (20) Shi, S. Biologics: an update and challenge of their pharmacokinetics. *Curr. Drug Metab.* **2014**, *15* (3), 271–90.
- (21) Morris, A. A.; Kozich, V.; Santra, S.; Andria, G.; Ben-Omran, T. I.; Chakrapani, A. B.; Crushell, E.; Henderson, M. J.; Hochuli, M.; Huemer, M.; Janssen, M. C.; Maillot, F.; Mayne, P. D.; McNulty, J.; Morrison, T. M.; Ogier, H.; O'Sullivan, S.; Pavlikova, M.; de Almeida, I. T.; Terry, A.; Yap, S.; Blom, H. J.; Chapman, K. A. Guidelines for the diagnosis and management of cystathionine beta-synthase deficiency. *J. Inherited Metab. Dis.* **2017**, *40* (1), 49–74.
- (22) Pasut, G.; Veronese, F. M. State of the art in PEGylation: the great versatility achieved after forty years of research. *J. Controlled Release* **2012**, *161* (2), 461–72.
- (23) Frank, N.; Kery, V.; Maclean, K. N.; Kraus, J. P. Solvent-accessible cysteines in human cystathionine beta-synthase: crucial role of cysteine 431 in S-adenosyl-L-methionine binding. *Biochemistry* **2006**, *45* (36), 11021–9.
- (24) Taoka, S.; Lepore, B. W.; Kabil, O.; Ojha, S.; Ringe, D.; Banerjee, R. Human cystathionine beta-synthase is a heme sensor protein. Evidence that the redox sensor is heme and not the vicinal cysteines in the CXXC motif seen in the crystal structure of the truncated enzyme. *Biochemistry* **2002**, *41* (33), 10454–61.
- (25) Baldo, B. A. Enzymes approved for human therapy: indications, mechanisms and adverse effects. *BioDrugs* **2015**, *29* (1), 31–55.
- (26) Shen, B. Q.; Xu, K.; Liu, L.; Raab, H.; Bhakta, S.; Kenrick, M.; Parsons-Reponte, K. L.; Tien, J.; Yu, S. F.; Mai, E.; Li, D.; Tibbitts, J.; Baudys, J.; Saad, O. M.; Scales, S. J.; McDonald, P. J.; Hass, P. E.; Eigenbrot, C.; Nguyen, T.; Solis, W. A.; Fuji, R. N.; Flagella, K. M.; Patel, D.; Spencer, S. D.; Khawli, L. A.; Ebens, A.; Wong, W. L.; Vandlen, R.; Kaur, S.; Sliwkowski, M. X.; Scheller, R. H.; Polakis, P.; Junutula, J. R. Conjugation site modulates the in vivo stability and therapeutic activity of antibody-drug conjugates. *Nat. Biotechnol.* **2012**, *30* (2), 184–9.
- (27) Sarkissian, C. N.; Gamez, A.; Wang, L.; Charbonneau, M.; Fitzpatrick, P.; Lemontt, J. F.; Zhao, B.; Vellard, M.; Bell, S. M.; Henschell, C.; Lambert, A.; Tsuruda, L.; Stevens, R. C.; Scriver, C. R. Preclinical evaluation of multiple species of PEGylated recombinant phenylalanine ammonia lyase for the treatment of phenylketonuria. *Proc. Natl. Acad. Sci. U. S. A.* **2008**, *105* (52), 20894–9.
- (28) Gamez, A.; Sarkissian, C. N.; Wang, L.; Kim, W.; Straub, M.; Patch, M. G.; Chen, L.; Striepeke, S.; Fitzpatrick, P.; Lemontt, J. F.; O'Neill, C.; Scriver, C. R.; Stevens, R. C. Development of pegylated forms of recombinant *Rhodospiridium toruloides* phenylalanine ammonia-lyase for the treatment of classical phenylketonuria. *Mol. Ther.* **2005**, *11* (6), 986–9.
- (29) Fee, C. J.; Van Alstine, J. A. PEG-proteins: Reaction engineering and separation issues. *Chem. Eng. Sci.* **2006**, *61* (3), 924–939.
- (30) Refsum, H.; Helland, S.; Ueland, P. M. Radioenzymic determination of homocysteine in plasma and urine. *Clin. Chem.* **1985**, *31*, 624–628.
- (31) Rasmussen, K.; Moller, J. Total homocysteine measurement in clinical practice. *Ann. Clin. Biochem.* **2000**, *37* (Pt 5), 627–48.
- (32) Jakubowski, H. The determination of homocysteine-thiolactone in biological samples. *Anal. Biochem.* **2002**, *308* (1), 112–9.
- (33) Mansoor, M. A.; Ueland, P. M.; Aarsland, A.; Svandal, A. Redox status and protein binding of plasma homocysteine and other aminothiols in patients with homocystinuria. *Metab. Clin. Exp.* **1993**, *42*, 1481–1485.
- (34) Bar-Or, D.; Curtis, C. G.; Sullivan, A.; Rael, L. T.; Thomas, G. W.; Craun, M.; Bar-Or, R.; Maclean, K. N.; Kraus, J. P. Plasma albumin cysteinylolation is regulated by cystathionine beta-synthase. *Biochem. Biophys. Res. Commun.* **2004**, *325* (4), 1449–53.
- (35) Boldt, J. Use of albumin: an update. *Br. J. Anaesth.* **2010**, *104* (3), 276–84.
- (36) Wraith, J. E. Limitations of enzyme replacement therapy: current and future. *J. Inherited Metab. Dis.* **2006**, *29* (2–3), 442–7.

# **SUPPORTING INFORMATION**

## **for**

### **Engineering and characterization of an enzyme replacement therapy for classical homocystinuria**

**Tomas Majtan,<sup>\*,†</sup> Insun Park,<sup>†</sup> Richard S. Carrillo,<sup>†</sup> Erez M. Bublil,<sup>‡</sup> and Jan P. Kraus<sup>\*,†</sup>**

<sup>†</sup>Department of Pediatrics, University of Colorado School of Medicine, Aurora, CO 80045, USA

<sup>‡</sup>Orphan Technologies Ltd., Rapperswil, CH-8640, Switzerland

\*To whom the correspondence should be addressed:

Dr. Tomas Majtan, University of Colorado School of Medicine, 12800 E 19<sup>th</sup> Ave, Mail Stop 8313,  
Aurora, CO, 80045, USA; tel: 303-724-3813, fax: 303-724-3838, e-mail:  
[tomas.majtan@ucdenver.edu](mailto:tomas.majtan@ucdenver.edu)

Dr. Jan Kraus, University of Colorado School of Medicine, 12800 E 19<sup>th</sup> Ave, Mail Stop 8313,  
Aurora, CO, 80045, USA; tel: 303-724-3812, fax: 303-724-3838, e-mail: [jan.kraus@ucdenver.edu](mailto:jan.kraus@ucdenver.edu)

**Supplementary Table S1. Maleimide PEGylation mapping – Lys-C digest.** Relative ratio of non-PEGylated cysteine-containing Lys-C peptides in each of the three proteins shown in **Supplementary Figure S1**. Red color indicates the peptide 272-322 containing C272 and C275 as differentially recovered after Lys-C digest indicating PEGylation.

Cys-containing Lys-C peptide	htCBS C15S	<i>homo</i> PEGylated 40MA PEG-CBS P1	<i>hemi</i> PEGylated 40MA PEG-CBS P2
40-72	0.40	0.36	0.40
103-108	0.05	0.04	0.04
109-119	0.07	0.06	0.07
120-172	0.15	0.13	0.14
212-247	0.21	0.20	0.21
272-322	0.25	0.08	0.17
326-359	0.14	0.12	0.13
360-384	0.12	0.11	0.12



**Supplementary Table S2. Maleimide PEGylation mapping – NTCB digest.** Relative ratio of representative five NTCB peptides in each of the three proteins shown in **Supplementary Figure S2**. Red color indicates that the C272 residue is blocked by PEGylation lowering the yield for the the 244-271 peptide in the *homo*PEGylated 40MA PEG-CBS P1 sample and to a lesser extent in the *hemi*PEGylated 40MA PEG-CBS P2.

NTCB peptide	htCBS C15S (ref)		<i>homo</i> PEGylated 40MA PEG-CBS P1			<i>hemi</i> PEGylated 40MA PEG-CBS P2		
	$\Delta$ mass (ppm)	relative abundance	$\Delta$ mass (ppm)	relative abundance	ratio ref:P1	$\Delta$ mass (ppm)	relative abundance	ratio ref:P2
<b>52-102</b>	-1.25	0.006	-1.92	0.0054	1.2	1.45	0.0054	1.2
<b>103-108</b>	-0.57	0.002	-1.86	0.0014	1.6	-3.00	0.0024	1.0
<b>244-271</b>	1.28	0.003	-0.90	<b>0.0011</b>	<b>2.7</b>	1.73	<b>0.0021</b>	<b>1.4</b>
<b>275-345</b>	0.76	0.001	0.64	0.0006	1.6	0.93	0.0007	1.4
<b>370-413</b>	0.67	0.045	-1.28	0.037	1.2	0.31	0.040	1.1

**Supplementary Table S3. NHS ester PEGylation mapping – peptides identified by LC/MS/MS from an Asp-N digest of reduced, alkylated, unmodified htCBS C15S (reference).**

Sequence Location	Sequence	Observed Modifications	Theoretical Mass (Da) <sup>a</sup>	Observed Mass (Da) <sup>b</sup>	$\Delta$ mass (ppm)	RT (min) <sup>c</sup>	Abundance <sup>d</sup>
A(2-34)	PSETPQAEVGPTGSPHRSGPHSAKGSLEKGSPE		3294.5865	3294.5886	0.64	33.8	462828
A(9-34)	EVGPTGSPHRSGPHSAKGSLEKGSPE		2584.2630	2584.2632	0.07	30.8	449108
A(35-46)	DKEAKEPLWIRP		1480.8038	1480.8037	-0.08	50.6	323088
A(40-46)	EPLWIRP		909.5072	909.5079	0.71	54.5	1369777
A(47-78)	DAPSRCTWQLGRPASESPHHHTAPAKSPKILP		3528.7797	3528.7802	0.13	49.0	1805933
A(79-85)	DILKKIG		785.5011	785.5011	0.06	41.9	1034520
A(86-106)	DTPMVRINKIGKKFGLKCELL		2459.3756	2459.3763	0.07	59.8	752660
A(107-119)	AKCEFFNAGGSVK		1413.6711	1413.6715	0.28	41.5	865418
A(120-128)	DRISLRMIE		1131.6070	1131.6079	0.74	51.3	1259968
A(120-128)	DRISLRMIE	1*Oxidation	1147.6019	1147.6023	0.34	43.8	42144
A(133-139)	DGTLKPG		686.3599	686.3604	0.72	24.0	665344
A(140-178)	DTIIEPTSGNTGIGLALAAAVRGYRCIIVMPEKMSS EKV		4147.1480	4147.1468	-0.29	92.2	422022
A(179-197)	DVLRALGAEIVRTPTNARF		2098.1647	2098.1652	0.21	64.2	3651887
A(179-197)	DVLRALGAEIVRTPTNARF	1*Deamidation	2099.1487	2099.1512	1.17	63.7	1401992
A(198-220)	DSPESHVGVAVRLKNEIPNSHIL		2597.3350	2597.3345	-0.20	58.1	1160943
A(198-220)	DSPESHVGVAVRLKNEIPNSHIL	1*Deamidation	2598.3191	2598.3195	0.17	58.8	543933
A(221-233)	DQYRNASNPLAHY		1547.7117	1547.7121	0.22	40.9	209797
A(221-233)	DQYRNASNPLAHY	1*Deamidation	1548.6957	1548.6982	1.59	40.3	156242
A(221-233)	DQYRNASNPLAHY	1*Deamidation	1548.6957	1548.6969	0.79	41.2	708853
A(238-244)	DEILQQC		904.3960	904.3961	0.12	33.1	258834
A(245-248)	DGKL		431.2380	431.2380	0.01	19.7	98742
A(249-269)	DMLVASVGTGGTITGIARKLK		2087.1773	2087.1773	0.04	59.3	458054
A(249-269)	DMLVASVGTGGTITGIARKLK	1*Oxidation	2103.1722	2103.1731	0.42	55.3	112910
A(270-301)	EKCPGCRIGVDPEGSILAEPEELNQTEQTTY		3632.6975	3632.6968	-0.18	57.7	99941

Sequence Location	Sequence	Observed Modifications	Theoretical Mass (Da) <sup>a</sup>	Observed Mass (Da) <sup>b</sup>	$\Delta$ mass (ppm)	RT (min) <sup>c</sup>	Abundance <sup>d</sup>
A(302-308)	EVEGIGY		765.3545	765.3552	0.99	38.3	356953
A(309-315)	DFIPTVL		803.4429	803.4429	-0.02	66.5	1980222
A(316-320)	DRTVV		588.3231	588.3236	0.75	27.3	891244
A(321-327)	DKWFKSN		923.4501	923.4502	0.03	35.3	209620
A(328-365)	DEEAFTFARMLIAQEGLLCGGSAGSTVAVAVKA AQELQ		3937.9554	3937.9544	-0.26	95.1	200461
A(333-348)	TFARMLIAQEGL		1735.8750	1735.8719	-1.79	47.2	212890
A(363-375)	ELQEGQRCVVILP		1539.8079	1539.8084	0.31	55.7	81479
A(366-375)	EGQRCVVILP		1169.6227	1169.6223	-0.36	53.8	375007
A(376-387)	DSVRNYMTKFLS		1459.7130	1459.7127	-0.15	55.3	1194612
A(388-400)	DRWMLQKGFLKEE		1678.8501	1678.8509	0.44	52.2	836829
A(388-400)	DRWMLQKGFLKEE	1*Oxidation	1694.8450	1694.8457	0.39	49.4	129978
A(401-413)	DLTEKKPWWHLR		1793.9366	1793.9369	0.19	56.7	2238451

<sup>a</sup> Theoretical molecular masses (mono-isotopic) were calculated using MassHunter BioConfirm software (Agilent, Santa Clara, CA)

<sup>b</sup> Observed masses (mono-isotopic) are all within 5 ppm of their theoretical value

<sup>c</sup> Retention time

<sup>d</sup> Abundances were determined using MassHunter software (Agilent, Santa Clara, CA)



**Supplementary Table S4. NHS ester PEGylation mapping – peptides identified by LC/MS/MS from an Asp-N digest of reduced, alkylated, PEGylated 20NHS PEG-CBS (batch #1).**

Sequence Location	Sequence	Observed Modifications	Theoretical Mass (Da) <sup>a</sup>	Observed Mass (Da) <sup>b</sup>	$\Delta$ mass (ppm)	RT (min) <sup>c</sup>	Abundance <sup>d</sup>	Estimated PEG/Peptide <sup>e</sup>
A(2-34)	PSETPQAEVGPTGSPHRSGPHSAKGSLEKGSPE		3294.5865	3294.5850	-0.46	33.8	74988	1.29
A(2-34)	PSETPQAEVGPTGSPHRSGPHSAKGSLEKGSPE	1*Linker	3408.6182	3408.6223	1.20	36.7	285758	
A(2-34)	PSETPQAEVGPTGSPHRSGPHSAKGSLEKGSPE	2*Linker	3522.6499	3522.6517	0.51	39.3	251006	
A(9-34)	EVGPTGSPHRSGPHSAKGSLEKGSPE		2584.2630	2584.2641	0.43	30.8	50722	1.03
A(9-34)	EVGPTGSPHRSGPHSAKGSLEKGSPE	1*Linker	2698.2947	2698.2983	1.34	34.6	156217	
A(9-34)	EVGPTGSPHRSGPHSAKGSLEKGSPE	2*Linker	2812.3264	2812.3276	0.43	37.6	59784	
A(35-46)	DKEAKEPLWIRP		1480.8038	1480.8040	0.14	50.5	419366	0.22
A(35-46)	DKEAKEPLWIRP	1*Linker	1594.8355	1594.8348	-0.42	53.3	115586	
A(40-46)	EPLWIRP		909.5072	909.5076	0.36	54.4	1267685	
A(47-78)	DAPSRCTWQLGRPAESP HHHTAPAK SPKILP		3528.7797	3528.7809	0.35	49.0	916229	0.37
A(47-78)	DAPSRCTWQLGRPAESP HHHTAPAK SPKILP	1*Linker	3642.8114	3642.8125	0.30	51.2	536395	
A(79-85)	DILKKIG		785.5011	785.5013	0.20	41.9	1447731	0.03
A(79-85)	DILKKIG	1*Linker	899.5328	899.5328	0.01	47.1	49654	
A(86-106)	DTPMVRINKIGKKFGLKCELL		2459.3756	2459.3756	0.00	59.8	278431	0.63
A(86-106)	DTPMVRINKIGKKFGLKCELL	1*Linker	2573.4073	2573.4078	0.20	63.4	207777	
A(86-106)	DTPMVRINKIGKKFGLKCELL	1*Linker	2573.4073	2573.4083	0.39	66.0	268441	
A(107-119)	AKCEFFNAGGSVK		1413.6711	1413.6714	0.21	41.5	1031048	
A(120-128)	DRISLRMIE		1131.6070	1131.6077	0.63	51.2	1738225	
A(120-128)	DRISLRMIE	1*Oxidation	1147.6019	1147.6017	-0.19	43.8	74835	
A(133-139)	DGTLKPG		686.3599	686.3603	0.53	24.0	837583	
A(140-178)	DTIIEPTSGNTGIGLALAAVRGYRCII VMPEKMSSEKV		4147.1480	4147.1479	-0.03	92.2	575055	

Sequence Location	Sequence	Observed Modifications	Theoretical Mass (Da) <sup>a</sup>	Observed Mass (Da) <sup>b</sup>	$\Delta$ mass (ppm)	RT (min) <sup>c</sup>	Abundance <sup>d</sup>	Estimated PEG/Peptide <sup>e</sup>
A(179-197)	DVLRALGAEIVRTPTNARF		2098.1647	2098.1651	0.18	64.1	4896736	
A(179-197)	DVLRALGAEIVRTPTNARF	1*Deamidation	2099.1487	2099.1500	0.59	63.6	1870150	
A(198-220)	DSPESHVGVAVRLKNEIPNSHIL		2597.3350	2597.3353	0.11	58.0	1302818	0.03
A(198-220)	DSPESHVGVAVRLKNEIPNSHIL	1*Deamidation	2598.3191	2598.3195	0.17	58.7	591137	
A(198-220)	DSPESHVGVAVRLKNEIPNSHIL	1*Linker	2711.3667	2711.3694	1.00	63.5	65301	
A(221-233)	DQYRNASNPLAHY		1547.7117	1547.7116	-0.06	40.9	256919	
A(221-233)	DQYRNASNPLAHY	1*Deamidation	1548.6957	1548.6975	1.11	40.3	198652	
A(221-233)	DQYRNASNPLAHY	1*Deamidation	1548.6957	1548.6967	0.61	41.2	802841	
A(238-244)	DEILQQC		904.3960	904.3957	-0.35	33.1	216368	
A(245-248)	DGKL		431.2380	431.2381	0.15	19.9	75839	0.49
A(245-248)	DGKL	1*Linker	545.2697	545.2695	-0.29	31.7	73171	
A(249-269)	DMLVASVGTGGTITGIARKLK		2087.1773	2087.1769	-0.18	59.2	458170	
A(249-269)	DMLVASVGTGGTITGIARKLK	1*Oxidation	2103.1722	2103.1725	0.16	55.2	130431	
A(270-301)	EKCPGCRIGVDPEGSILAEPEELNQTE QTTY		3632.6975	3632.7020	1.24	57.6	37257	0.39
A(270-301)	EKCPGCRIGVDPEGSILAEPEELNQTE QTTY	1*Linker	3746.7292	3746.7244	-1.28	59.5	23764	
A(302-308)	EVEGIGY		765.3545	765.3545	0.03	38.3	274612	
A(309-315)	DFIPTVL		803.4429	803.4431	0.29	66.4	2313422	
A(316-320)	DRTVV		588.3231	588.3232	0.11	27.2	1216696	
A(321-327)	DKWFKSN		923.4501	923.4502	0.03	35.3	100188	0.31
A(321-327)	DKWFKSN	1*Linker	1037.4818	1037.4812	-0.64	41.9	44718	
A(328-365)	DEEAFTFARMLIAQEGLLCGGSAGSTV AVAVKAAQELQ		3937.9554	3937.9538	-0.40	95.1	82719	
A(333-348)	TFARMLIAQEGL		1735.8750	1735.8718	-1.84	47.2	158013	
A(363-375)	ELQEGQRCVVILP		1539.8079	1539.8080	0.05	55.6	109572	
A(366-375)	EGQRCVVILP		1169.6227	1169.6229	0.17	53.7	425023	
A(376-387)	DSVRNYMTKFLS		1459.7130	1459.7135	0.34	55.2	1488072	
A(388-400)	DRWMLQKGFLKEE		1678.8501	1678.8500	-0.04	52.1	1018180	0.05
A(388-400)	DRWMLQKGFLKEE	1*Oxidation	1694.8450	1694.8450	-0.05	49.2	138406	

Sequence Location	Sequence	Observed Modifications	Theoretical Mass (Da) <sup>a</sup>	Observed Mass (Da) <sup>b</sup>	Δ mass (ppm)	RT (min) <sup>c</sup>	Abundance <sup>d</sup>	Estimated PEG/Peptide <sup>e</sup>
A(388-400)	DRWMLQKGFLKEE	1*Linker	1792.8818	1792.8812	-0.32	57.4	61595	
A(401-413)	DLTEKKPWWHLR		1793.9366	1793.9368	0.13	56.7	971171	0.74
A(401-413)	DLTEKKPWWHLR	1*Linker	1907.9683	1907.9684	0.08	60.8	1558334	
A(401-413)	DLTEKKPWWHLR	2*Linker	2022.0000	2022.0008	0.40	66.5	242737	

<sup>a</sup>Theoretical molecular masses (mono-isotopic) were calculated using MassHunter BioConfirm software (Agilent, Santa Clara, CA)

<sup>b</sup>Observed masses (mono-isotopic) are all within 5 ppm of their theoretical value

<sup>c</sup>Retention time

<sup>d</sup>Abundances were determined using MassHunter software (Agilent, Santa Clara, CA)

<sup>e</sup>The estimated number of PEG/peptide was calculated using the following formula:

$$\text{Estimated } \frac{\text{PEG}}{\text{peptide}} \text{ ratio} = \frac{(\text{Abundance}(1 * \text{Linker}) + 2 * \text{Abundance}(2 * \text{Linker}))}{\text{Abundance}(\text{No Linker}) + \text{Abundance}(1 * \text{Linker}) + \text{Abundance}(2 * \text{Linker})}$$

**Supplementary Table S5. NHS ester PEGylation mapping – peptides identified by LC/MS/MS from an Asp-N digest of reduced, alkylated, PEGylated 20NHS PEG-CBS (batch #2).**

Sequence Location	Sequence	Observed Modifications	Theoretical Mass (Da) <sup>a</sup>	Observed Mass (Da) <sup>b</sup>	$\Delta$ mass (ppm)	RT (min) <sup>c</sup>	Abundance <sup>d</sup>	Estimated PEG/Peptide <sup>e</sup>
A(2-34)	PSETPQAEVGPTGSPHRSGPHSAKGSLE KGSPE		3294.5865	3294.5858	-0.21	34.1	91654	1.06
A(2-34)	PSETPQAEVGPTGSPHRSGPHSAKGSLE KGSPE	1*Linker	3408.6182	3408.6173	-0.26	37.1	212552	
A(2-34)	PSETPQAEVGPTGSPHRSGPHSAKGSLE KGSPE	2*Linker	3522.6499	3522.6505	0.17	39.6	116731	
A(9-34)	EVGPTGSPHRSGPHSAKGSLEKGSPE		2584.2630	2584.2621	-0.35	31.2	110005	0.84
A(9-34)	EVGPTGSPHRSGPHSAKGSLEKGSPE	1*Linker	2698.2947	2698.2944	-0.10	35.0	207053	
A(9-34)	EVGPTGSPHRSGPHSAKGSLEKGSPE	2*Linker	2812.3264	2812.3283	0.68	37.6	50468	
A(35-46)	DKEAKEPLWIRP		1480.8038	1480.8040	0.15	51.1	130726	0.17
A(35-46)	DKEAKEPLWIRP	1*Linker	1594.8355	1594.8360	0.31	53.8	26208	
A(40-46)	EPLWIRP		909.5072	909.5075	0.31	54.9	370392	
A(47-78)	DAPSRCTWQLGRPASESPHHHTAPAKS PKILP		3528.7797	3528.7769	-0.79	49.4	608763	0.26
A(47-78)	DAPSRCTWQLGRPASESPHHHTAPAKS PKILP	1*Linker	3642.8114	3642.8084	-0.82	51.6	211918	
A(79-85)	DILKKIG		785.5011	785.5017	0.78	42.3	454812	0.02
A(79-85)	DILKKIG	1*Linker	899.5328	899.5338	1.11	47.5	11289	
A(86-106)	DTPMVRINKIGKKFGLKCELL		2459.3756	2459.3774	0.73	60.8	179277	0.54
A(86-106)	DTPMVRINKIGKKFGLKCELL	1*Linker	2573.4073	2573.4077	0.16	64.6	92660	
A(86-106)	DTPMVRINKIGKKFGLKCELL	1*Linker	2573.4073	2573.4068	-0.19	67.3	117060	
A(107-119)	AKCEFFNAGGSVK		1413.6711	1413.6716	0.35	42.0	495351	
A(120-128)	DRISLRMIE		1131.6070	1131.6075	0.46	51.7	664834	
A(120-128)	DRISLRMIE	1*Oxidation	1147.6019	1147.6023	0.35	44.3	33046	
A(133-139)	DGTLKPG		686.3599	686.3603	0.61	24.3	285635	
A(140-178)	DTIIEPTSGNTGIGLALAAVRGYRCIIV MPEKMSSEKV		4147.1480	4147.1451	-0.70	93.5	181549	



Sequence Location	Sequence	Observed Modifications	Theoretical Mass (Da) <sup>a</sup>	Observed Mass (Da) <sup>b</sup>	$\Delta$ mass (ppm)	RT (min) <sup>c</sup>	Abundance <sup>d</sup>	Estimated PEG/Peptide <sup>e</sup>
A(179-197)	DVLRALGAEIVRTPTNARF		2098.1647	2098.1657	0.49	65.3	2248724	
A(179-197)	DVLRALGAEIVRTPTNARF	1*Deamidation	2099.1487	2099.1508	0.99	64.8	936714	
A(198-220)	DSPESHVGVAVRLKNEIPNSHIL		2597.3350	2597.3345	-0.23	58.7	635630	0.02
A(198-220)	DSPESHVGVAVRLKNEIPNSHIL	1*Deamidation	2598.3191	2598.3202	0.45	59.5	352959	
A(198-220)	DSPESHVGVAVRLKNEIPNSHIL	1*Linker	2711.3667	2711.3649	-0.66	64.5	23552	
A(221-233)	DQYRNASNPLAHY		1547.7117	1547.7118	0.06	41.4	128480	
A(221-233)	DQYRNASNPLAHY	1*Deamidation	1548.6957	1548.6971	0.90	40.8	111326	
A(221-233)	DQYRNASNPLAHY	1*Deamidation	1548.6957	1548.6955	-0.17	41.7	405793	
A(238-244)	DEILQQC		904.3960	904.3962	0.23	33.5	126894	
A(245-248)	DGKL		431.2380	431.2381	0.12	20.5	40770	0.39
A(245-248)	DGKL	1*Linker	545.2697	545.2699	0.37	32.2	26289	
A(249-269)	DMLVASVGTGGTITGIARKLK		2087.1773	2087.1780	0.34	59.8	301153	
A(249-269)	DMLVASVGTGGTITGIARKLK	1*Oxidation	2103.1722	2103.1740	0.86	55.3	81381	
A(270-301)	EKCPGCRIGVDPEGSILAEPEELNQTEQ TTY		3632.6975	3632.6996	0.58	58.1	51146	0.27
A(270-301)	EKCPGCRIGVDPEGSILAEPEELNQTEQ TTY	1*Linker	3746.7292	3746.7269	-0.61	60.0	18541	
A(302-308)	EVEGIGY		765.3545	765.3549	0.49	38.7	244178	
A(309-315)	DFIPTVL		803.4429	803.4436	0.86	66.9	1102772	
A(316-320)	DRTVV		588.3231	588.3235	0.59	27.7	482942	
A(321-327)	DKWFKN		923.4501	923.4504	0.33	35.9	41312	0.21
A(321-327)	DKWFKN	1*Linker	1037.4818	1037.4826	0.77	42.5	10692	
A(328-365)	DEEAFTFARMLIAQEGLLCGGSAGSTV AVAVKAAQELQ		3937.9554	3937.9519	-0.89	95.6	35286	
A(333-348)	TFARMLIAQEGL		1735.8750	1735.8712	-2.19	47.7	113391	
A(363-375)	ELQEGQRCVVILP		1539.8079	1539.8083	0.26	55.9	44354	
A(366-375)	EGQRCVVILP		1169.6227	1169.6238	0.95	54.1	143135	

Sequence Location	Sequence	Observed Modifications	Theoretical Mass (Da) <sup>a</sup>	Observed Mass (Da) <sup>b</sup>	Δ mass (ppm)	RT (min) <sup>c</sup>	Abundance <sup>d</sup>	Estimated PEG/Peptide <sup>e</sup>
A(376-387)	DSVRNYMTKFLS		1459.7130	1459.7144	0.96	56.1	679328	
A(388-400)	DRWMLQKGFLKEE		1678.8501	1678.8505	0.22	52.8	428907	
A(388-400)	DRWMLQKGFLKEE	1*Oxidation	1694.8450	1694.8454	0.24	69.9	80607	0.04
A(388-400)	DRWMLQKGFLKEE	1*Linker	1792.8818	1792.8810	-0.45	58.2	20614	
A(401-413)	DLTEKKPWWHLR		1793.9366	1793.9372	0.38	57.6	638701	
A(401-413)	DLTEKKPWWHLR	1*Linker	1907.9683	1907.9691	0.45	62.1	633624	0.59
A(401-413)	DLTEKKPWWHLR	2*Linker	2022.0000	2022.0010	0.49	67.8	84315	

<sup>a</sup>Theoretical molecular masses (mono-isotopic) were calculated using MassHunter BioConfirm software (Agilent, Santa Clara, CA)

<sup>b</sup>Observed masses (mono-isotopic) are all within 5 ppm of their theoretical value

<sup>c</sup>Retention time

<sup>d</sup>Abundances were determined using MassHunter software (Agilent, Santa Clara, CA)

<sup>e</sup>The estimated number of PEG/peptide was calculated using the following formula:

$$\text{Estimated } \frac{\text{PEG}}{\text{peptide}} \text{ ratio} = \frac{(\text{Abundance}(1 * \text{Linker}) + 2 * \text{Abundance}(2 * \text{Linker}))}{\text{Abundance}(\text{No Linker}) + \text{Abundance}(1 * \text{Linker}) + \text{Abundance}(2 * \text{Linker})}$$

**Supplementary Table S5. NHS ester PEGylation mapping – peptides identified by LC/MS/MS from an Asp-N digest of reduced, alkylated, PEGylated 20NHS PEG-CBS (batch #3).**

Sequence Location	Sequence	Observed Modifications	Theoretical Mass (Da) <sup>a</sup>	Observed Mass (Da) <sup>b</sup>	$\Delta$ mass (ppm)	RT (min) <sup>c</sup>	Abundance <sup>d</sup>	Estimated PEG/Peptide <sup>e</sup>
A(2-34)	PSETPQAEVGPTGSPHRSGPHSAKGSLE KGSPE		3294.5865	3294.5829	-1.09	34.3	60072	1.24
A(2-34)	PSETPQAEVGPTGSPHRSGPHSAKGSLE KGSPE	1*Linker	3408.6182	3408.6154	-0.82	37.2	199290	
A(2-34)	PSETPQAEVGPTGSPHRSGPHSAKGSLE KGSPE	2*Linker	3522.6499	3522.6508	0.26	39.7	159538	
A(9-34)	EVGPTGSPHRSGPHSAKGSLEKGSPE		2584.2630	2584.2638	0.31	31.3	105797	0.98
A(9-34)	EVGPTGSPHRSGPHSAKGSLEKGSPE	1*Linker	2698.2947	2698.2940	-0.25	35.2	261221	
A(9-34)	EVGPTGSPHRSGPHSAKGSLEKGSPE	2*Linker	2812.3264	2812.3259	-0.18	37.6	96655	
A(35-46)	DKEAKEPLWIRP		1480.8038	1480.8039	0.09	51.3	86032	0.18
A(35-46)	DKEAKEPLWIRP	1*Linker	1594.8355	1594.8362	0.44	54.0	18790	
A(40-46)	EPLWIRP		909.5072	909.5078	0.62	55.0	395424	
A(47-78)	DAPSRCTWQLGRPAESP HHHTAPAKS PKILP		3528.7797	3528.7800	0.08	49.6	595498	0.31
A(47-78)	DAPSRCTWQLGRPAESP HHHTAPAKS PKILP	1*Linker	3642.8114	3642.8084	-0.81	51.7	272886	
A(79-85)	DILKKIG		785.5011	785.5017	0.81	42.5	446682	0.03
A(79-85)	DILKKIG	1*Linker	899.5328	899.5347	2.11	47.7	12609	
A(86-106)	DTPMVRINKIGKKFGLKCELL		2459.3756	2459.3745	-0.45	60.7	145186	0.61
A(86-106)	DTPMVRINKIGKKFGLKCELL	1*Linker	2573.4073	2573.4088	0.58	64.5	101537	
A(86-106)	DTPMVRINKIGKKFGLKCELL	1*Linker	2573.4073	2573.4057	-0.62	67.3	126416	
A(107-119)	AKCEFFNAGGSVK		1413.6711	1413.6721	0.71	42.2	506761	
A(120-128)	DRISLRMIE		1131.6070	1131.6075	0.42	51.9	725914	
A(120-128)	DRISLRMIE	1*Oxidation	1147.6019	1147.6020	0.04	44.3	29014	
A(133-139)	DGTLKPG		686.3599	686.3601	0.23	24.5	273520	
A(140-178)	DTIIEPTSGNTGIGLALAAVRGYRCIIV MPEKMSSEKV		4147.1480	4147.1398	-1.97	93.4	188751	

Sequence Location	Sequence	Observed Modifications	Theoretical Mass (Da) <sup>a</sup>	Observed Mass (Da) <sup>b</sup>	$\Delta$ mass (ppm)	RT (min) <sup>c</sup>	Abundance <sup>d</sup>	Estimated PEG/Peptide <sup>e</sup>
A(179-197)	DVLRALGAEIVRTPTNARF		2098.1647	2098.1663	0.73	65.2	2212569	
A(179-197)	DVLRALGAEIVRTPTNARF	1*Deamidation	2099.1487	2099.1511	1.12	64.7	930809	
A(198-220)	DSPESHVGVAVRLKNEIPNSHIL		2597.3350	2597.3339	-0.44	58.7	645205	0.03
A(198-220)	DSPESHVGVAVRLKNEIPNSHIL	1*Deamidation	2598.3191	2598.3196	0.20	59.5	348068	
A(198-220)	DSPESHVGVAVRLKNEIPNSHIL	1*Linker	2711.3667	2711.3668	0.04	64.4	31254	
A(221-233)	DQYRNASNPLAHY		1547.7117	1547.7124	0.48	41.7	119215	
A(221-233)	DQYRNASNPLAHY	1*Deamidation	1548.6957	1548.6981	1.56	41.1	113439	
A(221-233)	DQYRNASNPLAHY	1*Deamidation	1548.6957	1548.6959	0.14	42.0	404271	
A(238-244)	DEILQQC		904.3960	904.3962	0.16	33.7	137033	
A(245-248)	DGKL		431.2380	431.2384	0.93	20.8	41279	0.48
A(245-248)	DGKL	1*Linker	545.2697	545.2699	0.44	32.4	38708	
A(249-269)	DMLVASVGTGGTITGIARKLK		2087.1773	2087.1766	-0.32	59.8	378816	
A(249-269)	DMLVASVGTGGTITGIARKLK	1*Oxidation	2103.1722	2103.1743	1.00	55.3	81123	
A(270-301)	EKCPGCRIGVDPEGSILAEPEELNQTEQ TTY		3632.6975	3632.6934	-1.13	58.1	69301	0.29
A(270-301)	EKCPGCRIGVDPEGSILAEPEELNQTEQ TTY	1*Linker	3746.7292	3746.7248	-1.17	60.0	28571	
A(302-308)	EVEGIGY		765.3545	765.3551	0.76	39.0	267474	
A(309-315)	DFIPTVL		803.4429	803.4434	0.66	66.9	1030604	
A(316-320)	DRTVV		588.3231	588.3236	0.72	27.9	474399	
A(321-327)	DKWFKN		923.4501	923.4498	-0.30	36.3	46084	0.21
A(321-327)	DKWFKN	1*Linker	1037.4818	1037.4838	1.93	42.8	12212	
A(328-365)	DEEAFTFARMLIAQEGLLCGGSAGSTV AVAVKAAQELQ		3937.9554	3937.9541	-0.33	95.6	45366	
A(333-348)	TFARMLIAQEGL		1735.8750	1735.8700	-2.88	48.0	99444	
A(363-375)	ELQEGQRCVVILP		1539.8079	1539.8083	0.26	56.0	45283	
A(366-375)	EGQRCVVILP		1169.6227	1169.6233	0.52	54.1	162480	

Sequence Location	Sequence	Observed Modifications	Theoretical Mass (Da) <sup>a</sup>	Observed Mass (Da) <sup>b</sup>	Δ mass (ppm)	RT (min) <sup>c</sup>	Abundance <sup>d</sup>	Estimated PEG/Peptide <sup>e</sup>
A(376-387)	DSVRNYMTKFLS		1459.7130	1459.7127	-0.16	56.2	715580	
A(388-400)	DRWMLQKGFLKEE		1678.8501	1678.8503	0.08	53.0	430875	0.05
A(388-400)	DRWMLQKGFLKEE	1*Oxidation	1694.8450	1694.8452	0.12	50.2	71467	
A(388-400)	DRWMLQKGFLKEE	1*Linker	1792.8818	1792.8825	0.39	58.2	24688	
A(401-413)	DLTEKKPWWHLR		1793.9366	1793.9372	0.38	57.7	524828	0.71
A(401-413)	DLTEKKPWWHLR	1*Linker	1907.9683	1907.9690	0.38	62.0	701248	
A(401-413)	DLTEKKPWWHLR	2*Linker	2022.0000	2022.0014	0.69	67.6	130215	

<sup>a</sup>Theoretical molecular masses (mono-isotopic) were calculated using MassHunter BioConfirm software (Agilent, Santa Clara, CA)

<sup>b</sup>Observed masses (mono-isotopic) are all within 5 ppm of their theoretical value

<sup>c</sup>Retention time

<sup>d</sup>Abundances were determined using MassHunter software (Agilent, Santa Clara, CA)

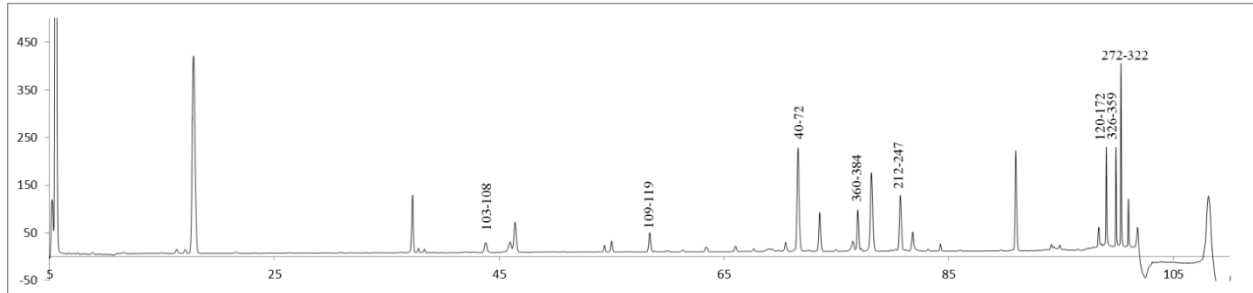
<sup>e</sup>The estimated number of PEG/peptide was calculated using the following formula:

$$\text{Estimated } \frac{\text{PEG}}{\text{peptide}} \text{ ratio} = \frac{(\text{Abundance}(1 * \text{Linker}) + 2 * \text{Abundance}(2 * \text{Linker}))}{\text{Abundance}(\text{No Linker}) + \text{Abundance}(1 * \text{Linker}) + \text{Abundance}(2 * \text{Linker})}$$

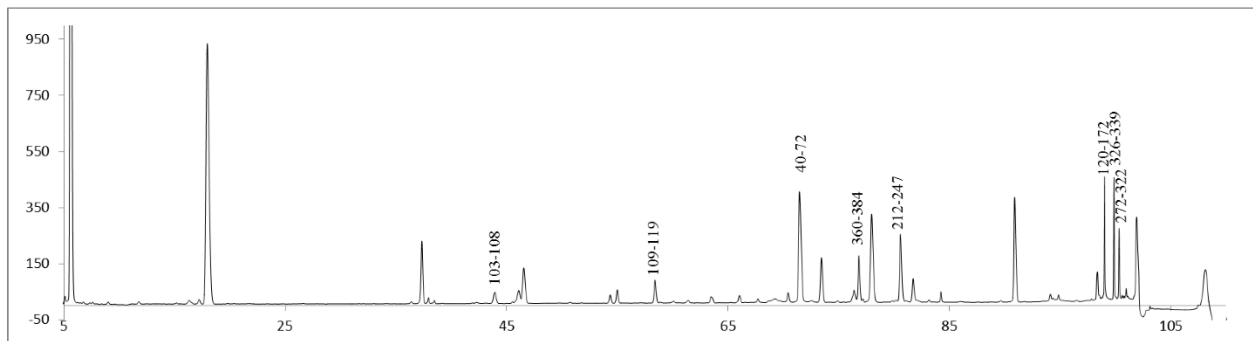


**Supplementary Figure S1. Maleimide PEGylation mapping – Lys-C digest.** Reduced alkylated LC-MS peptide maps after a Lys-C digest of unmodified htCBS C15S as a reference, *homo*PEGylated 40MA PEG-CBS P1 and *hemi*PEGylated 40MA PEG-CBS P2 proteins.

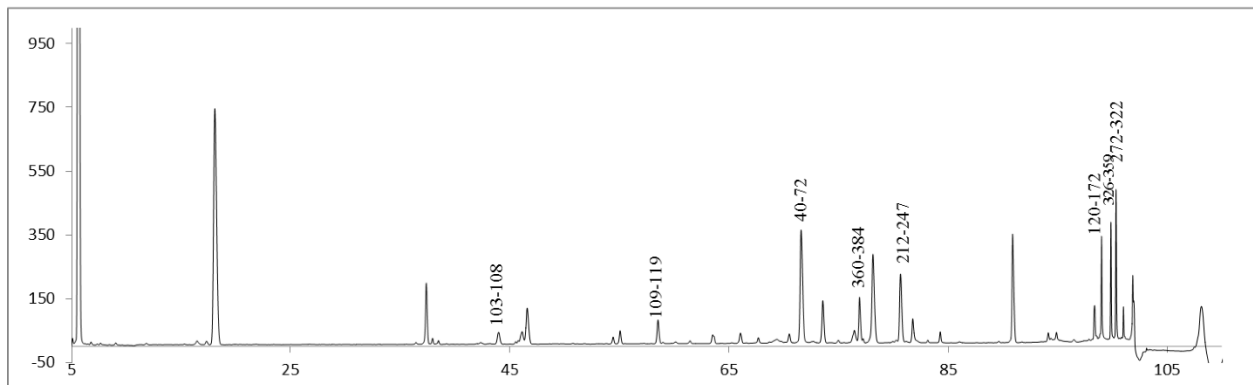
**htCBS C15S Lys-C digest (unmodified reference protein)**



**40MA PEG-CBS P1 Lys-C digest (*homo*PEGylated protein)**

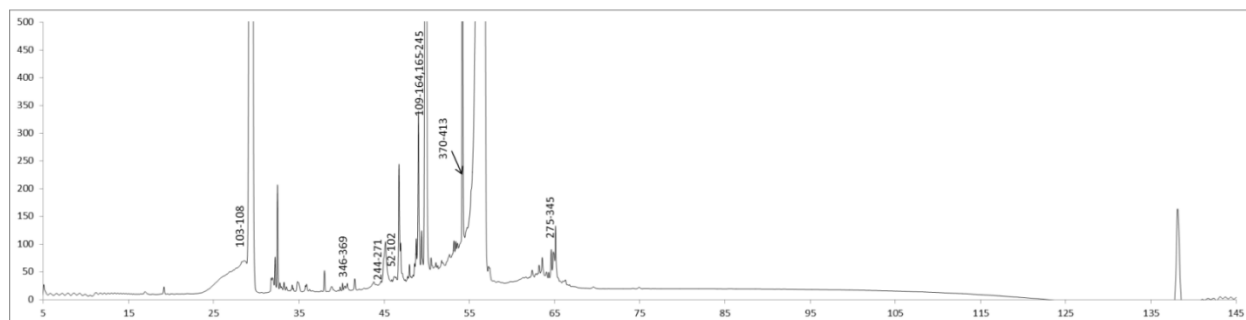


**40MA PEG-CBS P2 Lys-C digest (*hemi*PEGylated protein)**

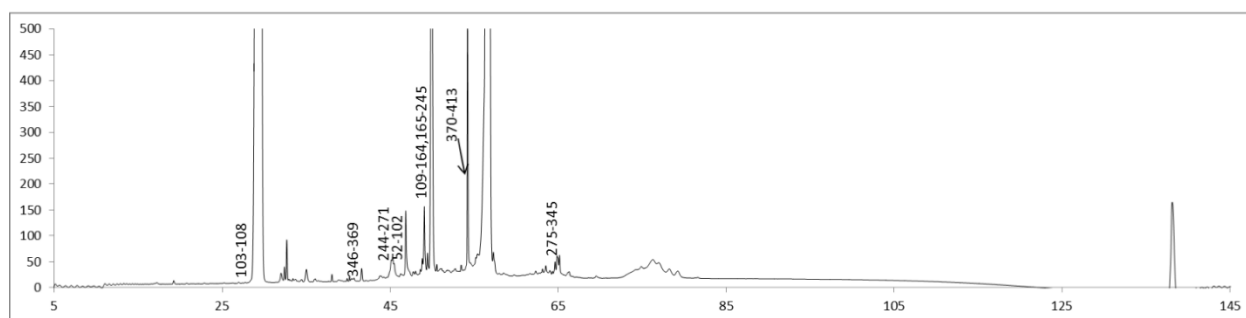


**Supplementary Figure S2. Maleimide PEGylation mapping – NTCB digest.** The LC-MS peptide maps after NTCB treatment of unmodified htCBS C15S as a reference, *homo*PEGylated 40MA PEG-CBS P1 and *hemi*PEGylated 40MA PEG-CBS P2 proteins.

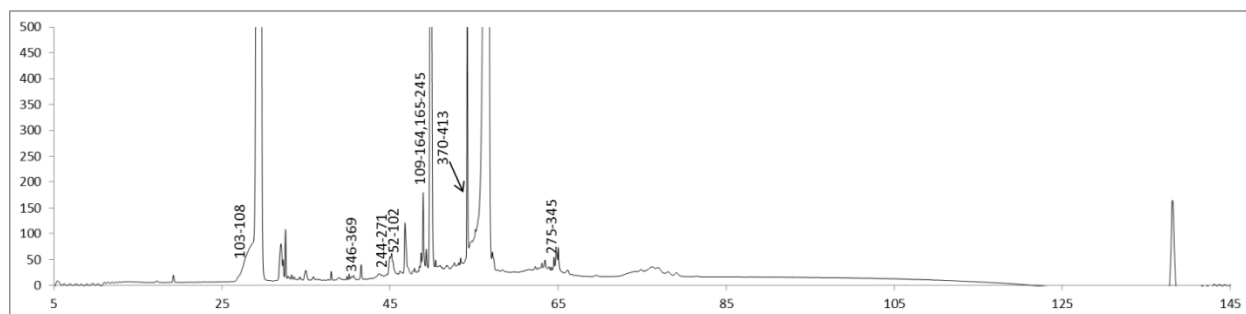
**htCBS C15S NTCB digest (unmodified reference protein)**



**40MA PEG-CBS P1 NTCB digest (*homo*PEGylated protein)**

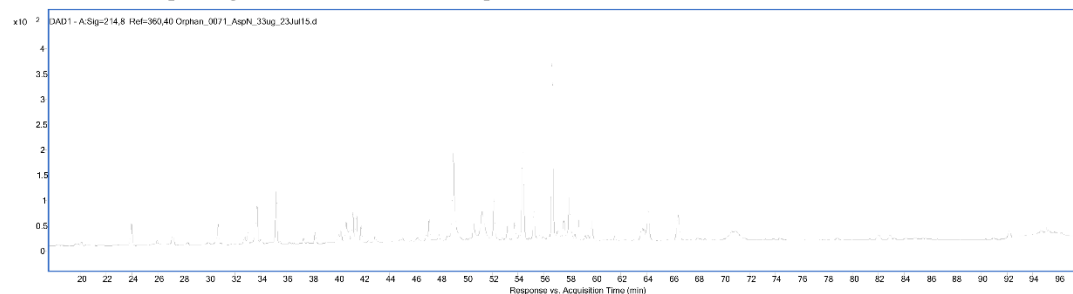


**40MA PEG-CBS P2 NTCB digest (*hemi*PEGylated protein)**

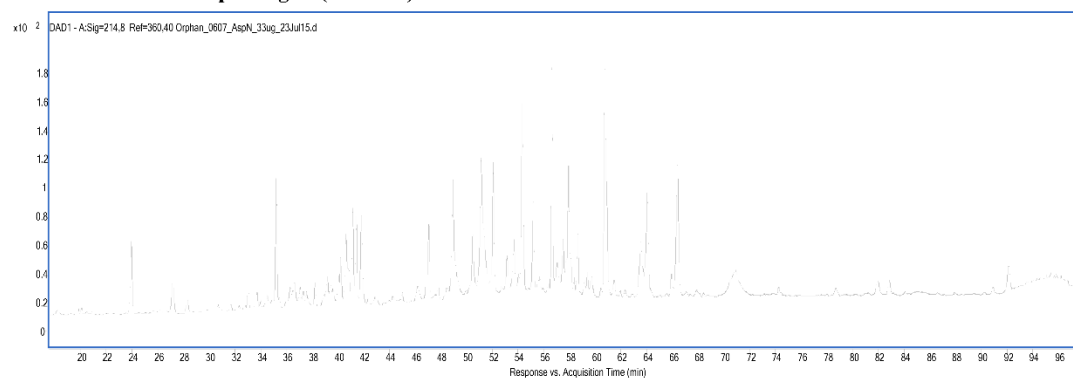


**Supplementary Figure S3. NHS ester PEGylation mapping.** The LC-MS peptide maps after Asp-N digest of unmodified htCBS C15S as a reference and three batches of 20NHS PEG-CBS.

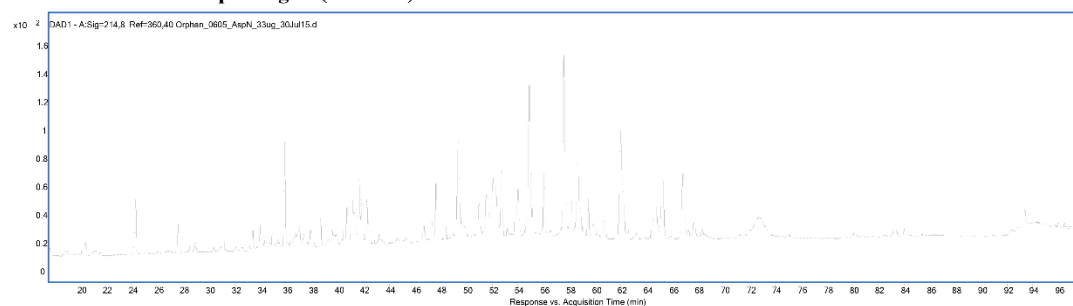
**htCBS C15S Asp-N digest (unmodified reference protein)**



**20NHS PEG-CBS Asp-N digest (batch #1)**



**20NHS PEG-CBS Asp-N digest (batch #2)**



**20NHS PEG-CBS Asp-N digest (batch #3)**

